Experimental evaluation of mutes in a car cd player

TU/e Eindhoven
Trainee-ship

Experimental evaluation of mutes in a car CD-player

R.A.C.M. Beerens

DCT 2001.51

This external trainee-ship has been performed at Philips Centre for Industrial Technology in Eindhoven. At the department acoustics and control in the group mechatronics research.

Professor: Prof. dr. H. Nijmeijer
Coach TU/e: Dr. ir. N. v.d. Wouw
Coach Philips: Dr. ir. M. Heertjes
Project leader: F. Cremers MSc

Faculty: Mechanical engineering
Group: Dynamics & control

Heythuysen, 5 October 2001

Preface

This trainee-ship doesn't stand for itself. For this reason experiences of others have been used, whom I would like to thank here.

These people are: Marcel Heertjes (coach CFT), Nathan van de Wouw (coach TU/e), Frank Cremers (project leader), Frank Sperling, Henk Neijmeijer, Ger Janssen, Dick Goossens, Gerard van Hattum, Lucas Koorneef and Kees van Tiel.

Without these people this part of the research-project wouldn't have succeeded.

Ruud Beerens

Summary

The performance of a CD-player is directly coupled to the level at which mutes (or dropouts) occur. This level is given as a function of the frequency and excitation amplitude of an applied harmonic force; this level will be denoted as the dropout level (DOL). To improve the performance (given by the level at which mutes occur) of a CD-player, it is important to find the cause for these mutes.
As a starting point for this project, the dropout level is taken to see whether there are any unexpected irregularities. This DOL is shown to be the inverse process sensitivity function of the closed-loop (the controlled) system. In this process sensitivity function, the radial error (the distance between the lens and the track to be followed) is regarded with respect to external disturbances. By studying the DOL-curve, an irregularity can be found between 40 [Hz] and 60 [Hz] with respect to the shape of the inverse process sensitivity function; this irregularity will be denoted as the dip. Also a dip in the maximum radial error is seen in this same range of frequencies. With this in mind the dynamics of the optical pick-up unit (opu), both in the uncontrolled and in the controlled situation, are studied, which is described in chapter 3.
In this chapter first the dynamics of the opu for the uncontrolled case are studied (open-loop), where it is found that the radial natural frequency (being about 34 [Hz]) of the opu suspension is in the vicinity of the dip (measured in the uncontrolled case). To investigate whether impact (between the optical pick-up unit and the side of the sledge) is the cause for the observed DOL irregularity, a collision detection mechanism (CDM) has been constructed. With the CDM, the occurrence of impact in the uncontrolled case has been proven. It has also been shown, that the CDM doesn't affect the controlled case, with respect to the DOL, in the frequency range of the irregularity.
To study a possible relationship between the uncontrolled (the natural frequency of the opu suspension) and the controlled (the DOL, especially the dip) case, it was tried to influence the uncontrolled dynamics of the opu. To do so, two possibilities have been considered, changing the mass of the opu and changing the stiffness of the suspension between the opu and the sledge. With additional mass, unexpected results are found in the uncontrolled case, which makes the measurements for the controlled case less valuable. Additional stiffness of the suspension between the opu and the sledge, however, yielded in the uncontrolled case the expected result. In the controlled case, the dip shifts with the natural frequency. A drawback of increasing the stiffness of the suspension of the opu is that it is unknown what happens to the tilt-mode of the opu (this is a torsion-mode of the opu, which is found around 43 [Hz] when no stiffness is added). The idea that the tilt-mode causes dropout is related to a dip found in the maximum radial error (the horizontal distance between the lens and the track). To see whether this mode has any influence on the system, a bridge construction is used. The goal of this construction is to suppress the tilt-mode, without influencing the translational dynamics (both in radial and in focus direction). With the construction, the dip in the DOL-curve disappeared, however, together with the impact in the uncontrolled situation. Probably the construction has also influenced the radial and the focus direction.
In chapter 4 the sledge dynamics are evaluated. It is found that the sledge suspension, especially the part between the nut and the sledge, has rather large relative amplitudes with respect to the excitation level at its natural frequency. This is why this part of the suspension has been stiffened, which results in an increase of the performance of the CD-player of 30% to 50% above an excitation frequency of 60 [Hz]. A closer inspection of the measurements above 60 [Hz], revealed a 3150 [Hz] frequency component in the radial error signals right before mute. Furthermore, it was found that when another track is played, this frequency-component shifts from 3150 [Hz] (track 1) to 2400 [Hz] (track 10).

Contents

1. Introduction

To increase the comfort of a driver (and its occupants) in a vehicle, APM-Wetzlar (Automotive Playback Modules in Wetzlar, Germany) studies the behaviour of CD-players in a vehicle. To specify the performance of a CD-player in a vehicle, they investigate the behaviour of a CD-module exposed to an external harmonic force. Especially the frequency-range between 0 [Hz] and 200 [Hz] is of interest, because this range covers the main contributions in vehicle vibrations; for example due to periodic disturbances of the road-surface or due to disturbances within the vehicle itself (the slam of a door or a beat on the dashboard).
Nowadays CD-players encompass a wide variety of linear and non-linear phenomena (e.g. optical pick-up unit-modes, sledge dynamics, pretension, cleavage, etcetera). Since the control design is based on linear feedback and/or feedforward techniques, non-linear phenomena, aside from unmodeled linear dynamics, are expected to limit the attainable performance.
The performance is given by the level of disturbance at which the module loses track. Track loss will either result in a mute, i.e. the lens loses track but is able to recover and will keep on playing; or it will result in a dropout, i.e. the lens is not able to recover track and the module will stop playing. In this thesis, two sub-goals will be studied in detail:

1. Which mechanisms cause mute and, subsequently:
2. Which mutes yield dropout.

This study will mainly be performed on a lab-scale set-up of a CD-player.
In chapter 2, this lab-scale set-up is studied. This with respect to the hardware (CD-module, sensors, etcetera) and to the software (controllers, measurements, data acquisition, etcetera). Also in this chapter, the starting point for this project is found, being the dropout level (DOL). This DOL is the level at which dropouts occur as a function of the external harmonic force offered. Furthermore, it will be shown that this DOL has the shape of the inverse process sensitivity function with an irregularity.
With respect to non-linear dynamics, this study will mainly focus on impact encountered between opu and sledge. In chapter 3, it will be shown that impact between opu and sledge can occur in the controlled case, which almost certainly results in mute. Besides, impact resulting from the uncontrolled opu dynamics, may difficult the recovery-time after mute, which can be the reason for the observation that mute related to impact almost certainly results in dropout.
In chapter 4, other reasons for mute will be studied. The main focus will be the sledge dynamics and how to improve (if possible) it by influencing the uncontrolled dynamics of the suspension.
Finally, in chapter 5, conclusions and recommendations are given.

2. Experimental set-up

In this chapter, the lab-scale set-up will be studied. Not only the hardware, but also the software will be regarded. At the end of the chapter some experiments will be done which form the basis of this study.

2.1 THE HARDWARE

In figure 2.1 the lab-scale experimental set-up is shown.

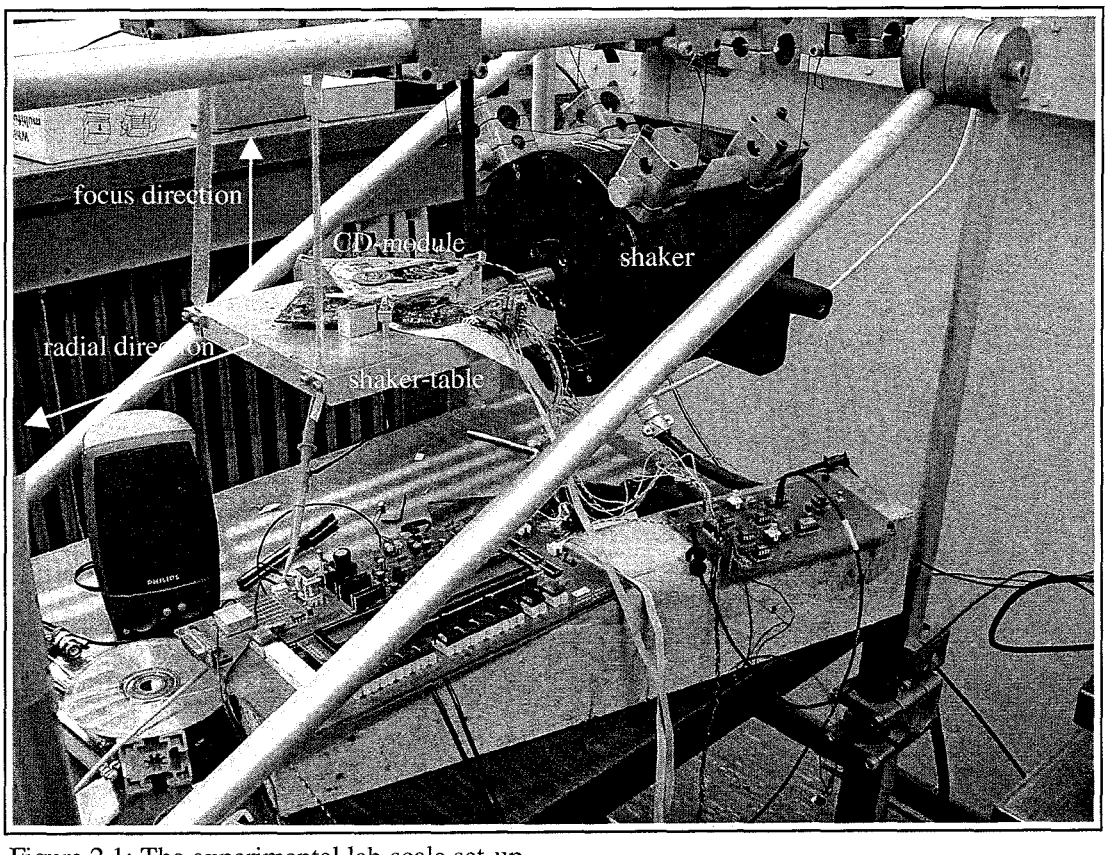

Figure 2.1: The experimental lab-scale set-up.

As can be seen in figure 2.1, the CD-player is mounted on top of the shaker-table, which is connected by wires to the world. It should be noted that the table has been aligned mechanically, so that it is merely excited in radial direction (horizontal plane). At the right of the table, the shaker, which applies the external harmonic load, is shown. Specifications of the shaker are given in appendix A1. For further understanding, a schematic presentation of the set-up is shown in figure 2.2, this also with respect to the possible in- and output signals.

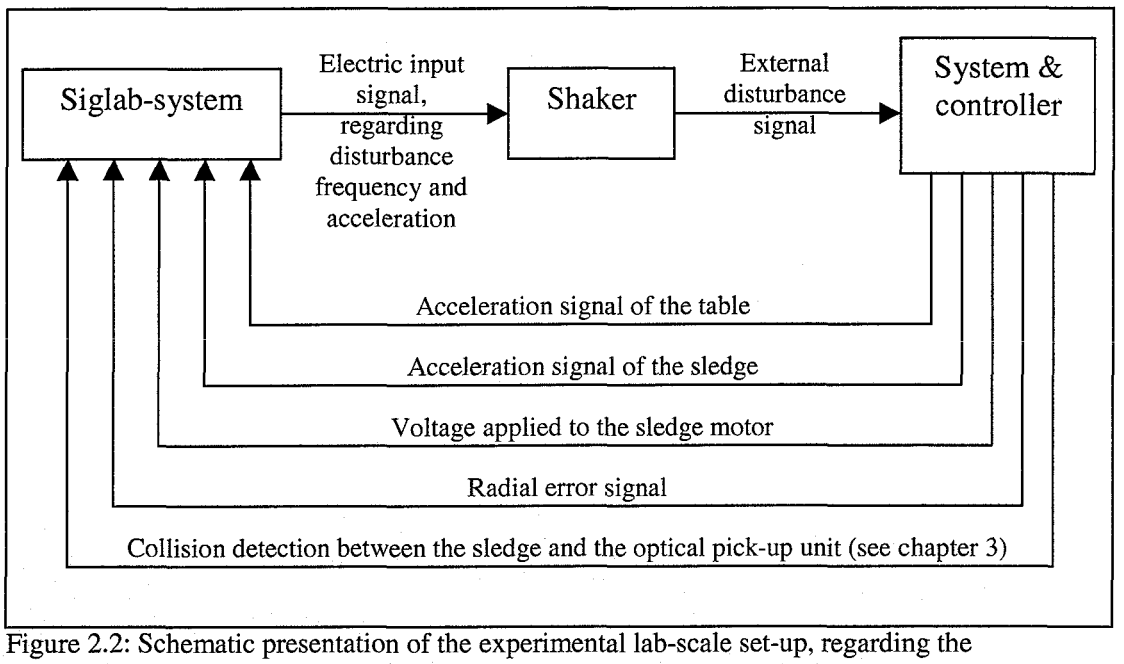

Figure 2.2: Schematic presentation of the experimental lab-scale set-up, regarding the possible in- and output signals. For further insight in the hardware of the CD-module, the reader is referred to figure 4.1.

The CD-module is divided into five main parts, which are important for this study: the disc turntable (and its motor), the optical pick-up unit (abbreviated as opu), the sledge, the transmission of the sledge and the sledge motor. In figure 2.3 a schematic representation of these parts are shown. The transmissions and suspensions between the different parts are represented as springs, *k*. In figure 2.4, these parts are shown within the module itself.

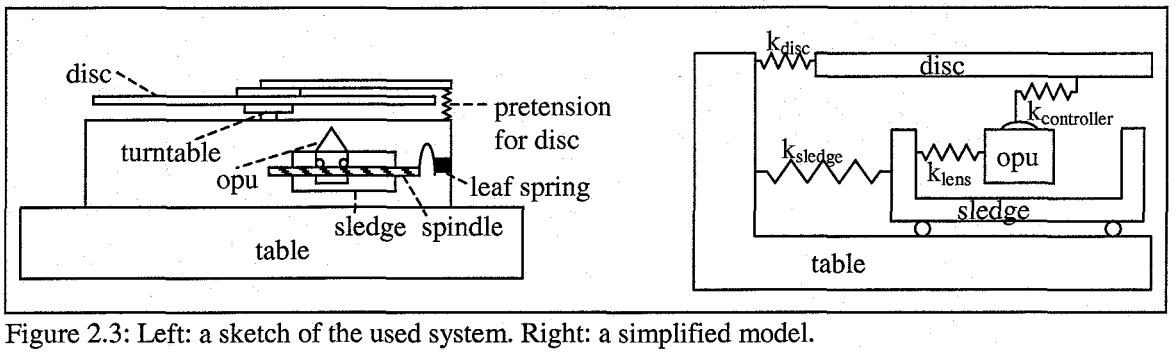

Figure 2.3: Left: a sketch of the used system. Right: a simplified model.

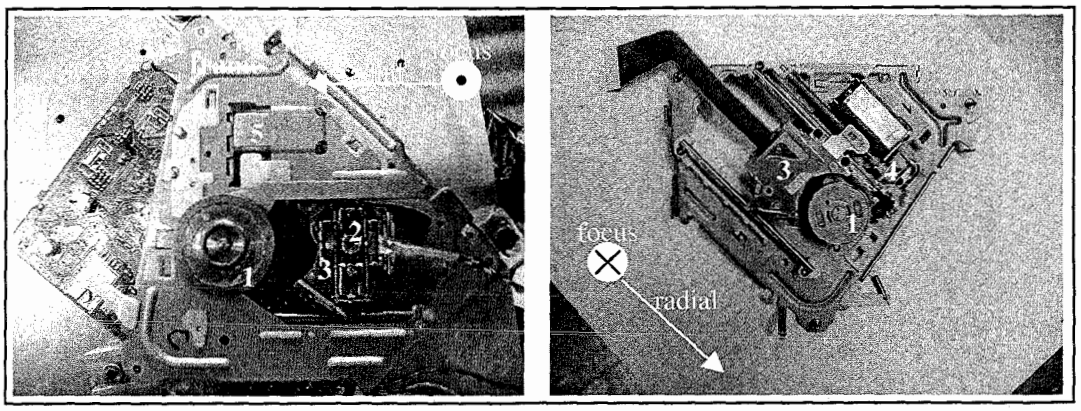

Figure 2.4: CD-player with: 1. Disc turntable; 2. Optical pick-up unit (opu); 3. Sledge; 4. Transmission of the sledge; 5. Sledge motor.

The turntable is responsible for the rotation of the disc. The disc has a mass of $15 \cdot 10^{-3}$ [kg]. Its tracks can be represented as a single spiral, usually centred outside the centre of rotation.

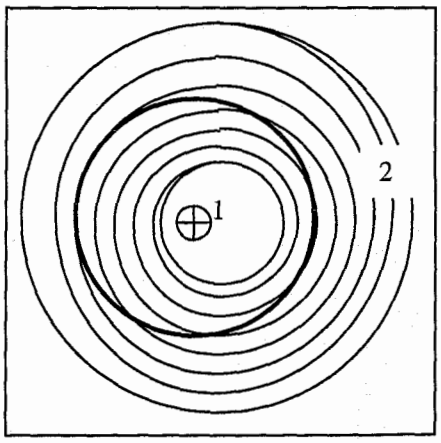

Figure 2.5: Schematic representation of the eccentricity of the tracks (2) with respect to the centre of the disc (1). The bold circle represents the trajectory of the lens, when it is not controlled.

The information density on a disc is distributed homogeneously. So, to uphold a constant information rate (which means that a constant linear velocity is necessary), the rotation velocity varies along the disc radius, i.e. about 22 [rad/s] for the outer track (the last track) and about 47 [rad/s] for the inner track (the first track).
The lens is a part of the opu, which also contains three sets of coils and four wires (as can be seen in figure 2.6). Besides opu support, these wires enable power transfer to the coils. The coils together with the magnets and soft iron cores form the actuator of the opu, and enable the generation of forces on the opu. These forces allow for relative displacement between opu and sledge in both radial and focus direction.

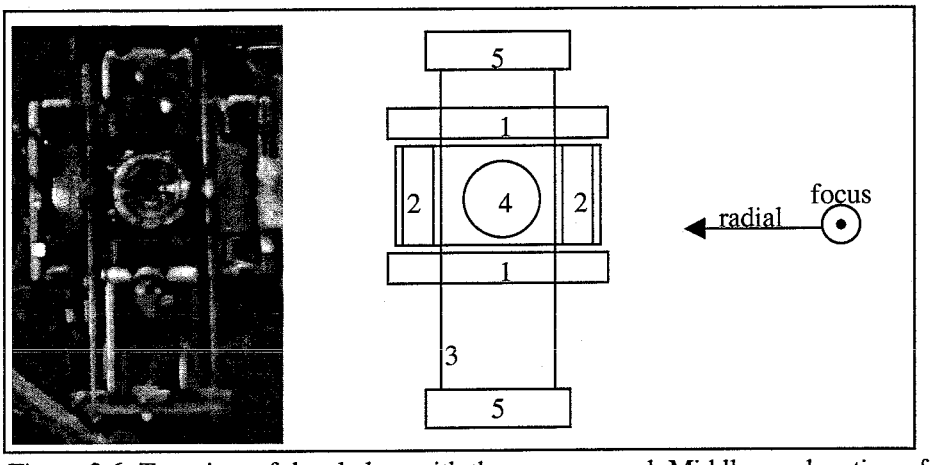

Figure 2.6: Top view of the sledge, with the cap removed. Middle: explanation of the left, with: 1. Magnet; 2. Coil; 3. Wire; 4. Lens; 5. Holder.

The sledge has a mass of $12 \cdot 10^{-3}$ [kg]. It is actuated by an electromotor, which assures the sledge to move (with a step) whenever the opu comes near its boundary, defined by the inner housing of the sledge. Gears, spindle and nut together form the coupling between the electromotor and the sledge. The spindle is pretensioned by a leaf spring, as can be seen in figure 2.7.

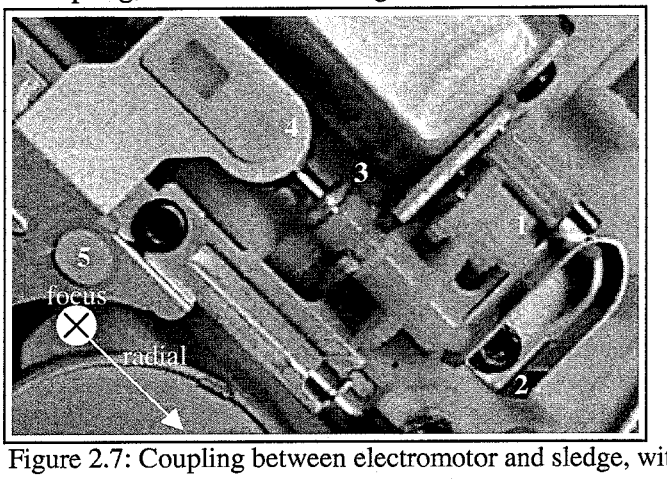

Figure 2.7: Coupling between electromotor and sledge, with: 1. Gears; 2. Leaf spring; 3. Spindle; 4. Nut; 5. Sledge.

2.2 THE SOFTWARE

The CD-player is controlled in a two-step approach. In the first step the opu is controlled by a PID-controller with both a high pass- and a low pass filter. Typically, the bandwidth is set at 1400 [Hz]. The breakpoint of the integral action can be found near 1/10 of the bandwidth, i.e. at about 140 [Hz], whereas the breakpoint of the differential action can be found near 1/3 of the bandwidth. The high-frequency roll-off is found near five times the bandwidth. The working area of the controller is limited by the cleavage between opu and sledge. Therefore, in the second step, the sledge is controlled on a much slower time-scale. The overall control scheme is given in figure 2.8.

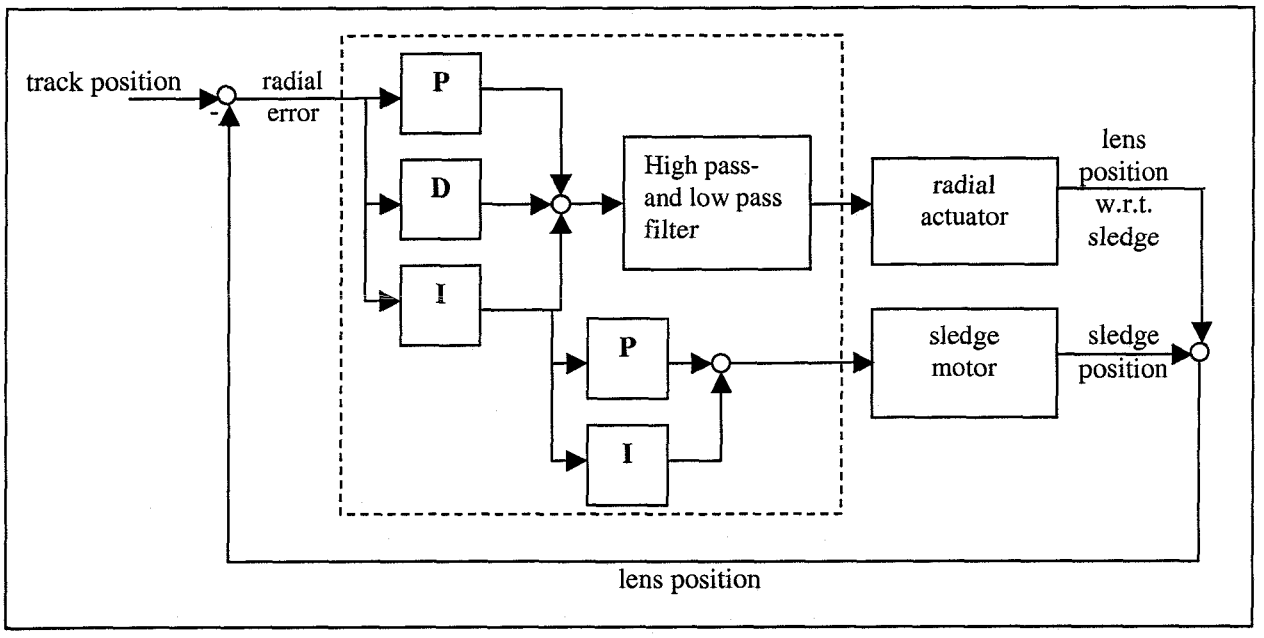

Figure 2.8: Block-diagram of the system. In the dashed part the used radial controller for the radial actuator and the sledge motor is shown.

Besides the radial loop, the opu is also controlled in focus direction. The focus control loop has a similar PID-structure as the radial loop, but will not be considered in this thesis, because the radial direction is the most sensitive direction for disturbances. Consequently, the occurrence of mute and dropout is expected to correspond to this direction only.

With the lab-scale setup, a so-called dropout level (abbreviated as DOL) measurement can be performed in order to retrieve the CD-player's performance. This DOL is a function of frequency and acceleration amplitude of the external excitation. Dropouts are detected by monitoring the radial error signal, using a siglab system (data acquisition system, including scope, function generator and analyser). This system is able to process four output signals and two input signals, of which one will be used to control the shaker. The siglab-system is able to produce many sorts of mathematical input signals. In this project only the sine- and the chirp-function (this function covers a wide domain of frequencies, 0 [Hz] to $20 \cdot 10^3$ [Hz]). In both functions the frequency and amplitude can be adjusted. The voltage measurement, representing the radial error, has been calibrated from an open-loop eccentricity measurement; see figure 2.9.

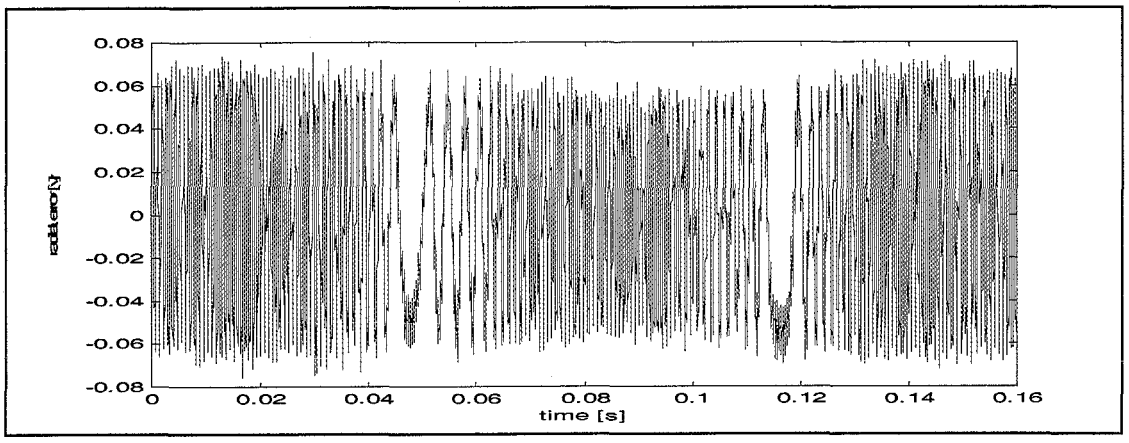

Figure 2.9: Experimental results regarding the factor of conversion with respect to the radial error.

From these experiments, it follows that the distance between two subsequent tracks of $1.6[\mu m]$ is given by 0.06 [volts], so 1 [volts] complies to $14[\mu m]$.

Aside from the radial error, four other measurements are possible (as already shown in figure 2.2), which are:

1. Two acceleration measurements, one used to measure the acceleration of the shaker-table and one to measure the acceleration of the sledge;
2. The voltage applied to the motor of the sledge, which is taken from the input of the motor voltage;
3. The detection of collisions between the opu and the sledge. A collision detection mechanism is made, which is described in chapter 3 and appendix 2.

Other measurements, which might be useful (but weren't possible to measure), are:

4. The focus error, which is the distance between the track and the lens (with a certain offset);
5. The audio signal, which simplifies the detection of a mute (now this is done by looking at the radial error).

To improve the correctness of the measurements, the acceleration meters are frequently calibrated.

2.3 THE DROPOUT LEVEL

The dropout level (DOL) is determined experimentally and depicted in figure 2.12. Basically, it shows the maximal acceleration of the disturbance (in the lab-scale set-up actuated by the shaker and in the vehicle by the road surface for example) at a certain frequency by which the CD-player will fall out of operation. Its shape may be explained by the inverse process sensitivity function (the transfer between radial error, e_{rad}, and the applied disturbance force, F) of the radial error loop. In figure 2.10, a schematical view of the radial error loop is given.

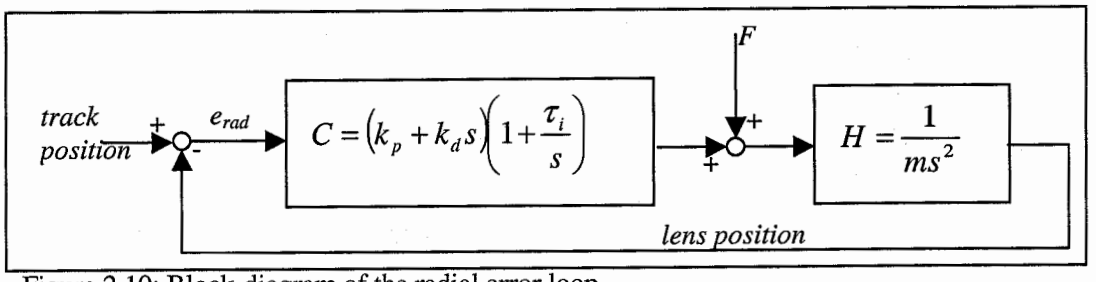

Figure 2.10: Block-diagram of the radial error loop.

For this block-diagram, the process sensitivity function in closed-loop yields:

$$\frac{e_{rad}}{F} = \frac{-H}{1+CH} \equiv \frac{-s}{ms^3 + (k_p + k_d s)(s + \tau_i)} \qquad [2.1]$$

The DOL is expected to be the inverse of this process sensitivity, which yields expected asymptotes, as given by figure 2.11.

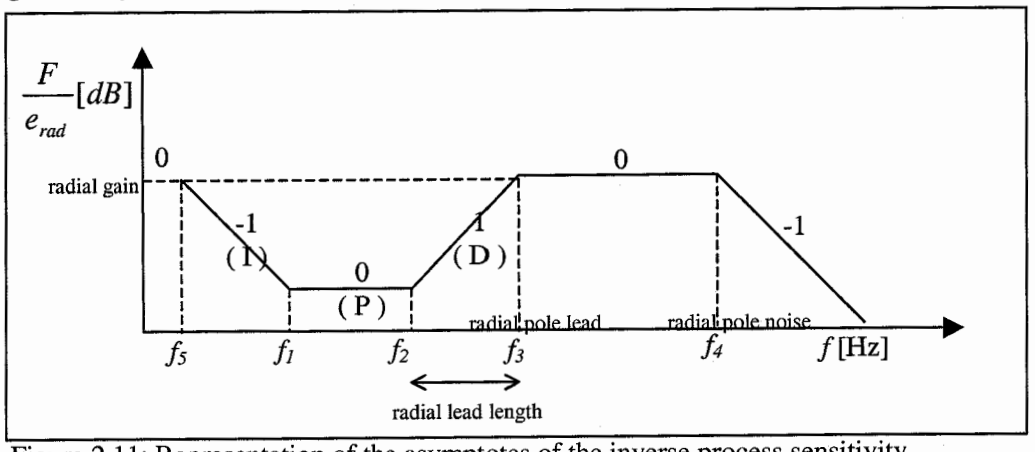

Figure 2.11: Representation of the asymptotes of the inverse process sensitivity function. The values in the figure are the values for the slopes in dB/decade. The denoted frequencies are: f_1 = radial integrator bandwidth; f_2 = begin of radial lead; f_3 = end of radial lead; f_4 = low pass function following PID; f_5 = integrator strength ($=f_1f_2/f_3$).

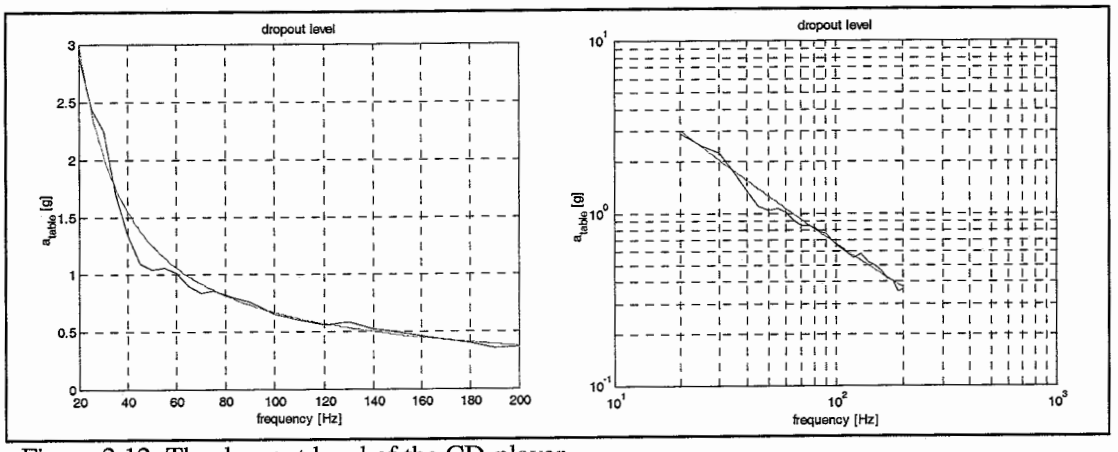

Figure 2.12: The dropout level of the CD-player.

In figure 2.12, it can be seen that this hypothesis reasonably matches with the measurements. It is also mentioned, that only the first asymptote (I-action) is used for the fit, since the breakpoint of this action is near 1/10 (at about 140 [Hz]) of the bandwidth (which is located at about 1400 [Hz]). However, at a certain frequency-range, large deviations occur, e.g. between 40 [Hz] and 60 [Hz] (this is also measured in CTB593-00-4174). These deviations form the basis of this thesis, because they most likely are related to unmodeled dynamics, which can be linear and/or non-linear. To find out more about these deviations from the expected inverse process sensitivity shape, both the dynamics of the opu and the sledge will be studied in more detail (both in the controlled and the uncontrolled case).

3. Non-linear lens dynamics (the optical pick-up unit)

As mentioned in the introduction, deviations in the dropout level-curve (DOL-curve, figure 2.12) with respect to the expected shape obtained from the inverse process sensitivity function will be studied in this chapter. Especially, the dip between 40 [Hz] and 60 [Hz], which will be related to non-linear opu (optical pick-up unit) dynamics. Namely, due to a change in stiffness with respect to the suspension of the opu an area of coexisting, stable solutions can be obtained in the frequency-domain. This area of coexistence (uncontrolled) corresponds to the frequency-area where the dip (controlled) is located. The phenomenon of coexisting, stable solutions will be explained in paragraph 3.1; for more theoretical background the reader is referred to appendix 3.
First, the uncontrolled opu dynamics will be studied from an experimental point of view. The non-linear impact dynamics will be of special interest. Second, a collision detection mechanism (CDM) will be made and the measurements, obtained using this device, will be discussed. It will be shown that impact between opu and sledge also occurs in the controlled case in this frequency-range between 40 [Hz] and 60 [Hz]. Third, the implications with respect to mute will be studied. Finally, mechanical changes are made to influence the dropout level (DOL) dip.

3.1 THE UNCONTROLLED OPU DYNAMICS

The uncontrolled opu dynamics merely consists of an opu mass ($7 \cdot 10^{-4}$ [kg]), a radial stiffness (32.34 [N/m]), a radial damping (0.0217 [N·s/m]) and a double-sided motion limitation represented by a cleavage of $\approx 0.5 \cdot 10^{-3}$ [m] per side. These specifications are given by the manufacturer. The natural frequency is given by:

$$f_n = \frac{1}{2\pi}\sqrt{\frac{k}{m}} = 34.2[Hz] \qquad [3.1]$$

In the vicinity of this frequency, the opu undergoes (see again figure 2.5) large vibrations and is, therefore, expected to exceed the available cleavage. Consequently, the response will no longer be linear, but will contain either motion with or without impact. This is shown in figure 3.1, while shaking the table in radial direction with acceleration amplitudes of 0.9 [g] and 1.9 [g] respectively.

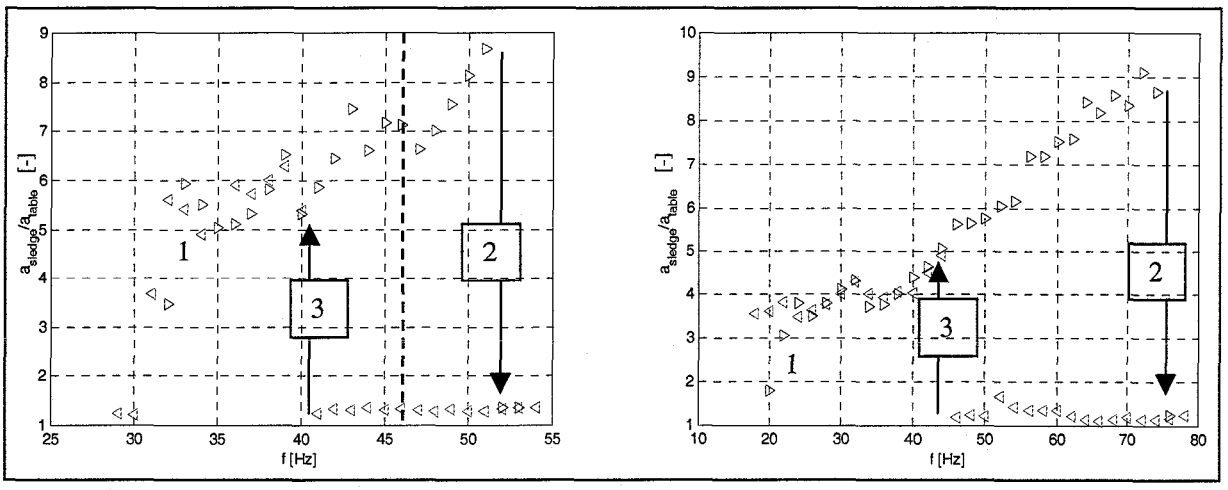

Figure 3.1: Coexisting solutions in the uncontrolled case, resulting from the non-linear opu dynamics from the suspension of the opu. The blue triangles represent a frequency increase, whereas the green ones represent a frequency decrease. Left: 0.9 [g]. Right: 1.9 [g].

In figure 3.1, the triangles represent the ratio between the maximum acceleration levels measured on the sledge and measured on the table for varying excitation frequency. Note that when no impact occurs, this ratio is expected to be almost one. This is expected because the natural frequency of the sledge suspension is expected at 650 [Hz] (see chapter 4), so below this frequency the frequency response function (between the acceleration of the table and the acceleration of the sledge) is expected to be valued at one. In the case of impact, however, large acceleration spikes measured on the sledge will drive this ratio to large values. The triangles show the direction of the frequency variation (blue represents a frequency increase and green a frequency decrease). If the frequency is increased the opu starts to impact on the sledge (point *1*); note that the acceleration ratio increases. Upon a certain frequency (point *2*), impact stops and the acceleration ratio instantly drops. When the frequency is now decreased, impacts will start at a much lower excitation frequency (point *3*). So between point *2* and *3*, at least two periodic responses coexist, one with and one without impact. These impacts can be heard. Which of the responses will be measured in practice depends on the initial conditions.
In figure 3.2, two coexisting responses at an excitation frequency of 46 [Hz] and at an acceleration level of 0.9 [g] have been depicted by the time-series of the acceleration measured on the sledge; see also the left part of figure 3.1 at 46 [Hz].

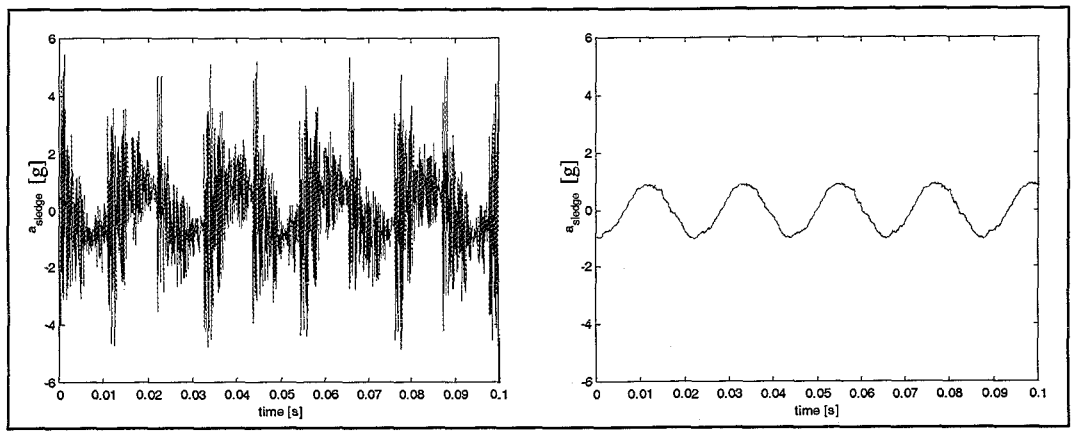

Figure 3.2: Two stable, coexisting solutions at an excitation of 46 [Hz] and an excitation level of 0.9 [g].

It can be seen that the sledge undergoes a large difference in motion when vibrating in one of these responses. This difference is caused by large sudden increases in the acceleration measurements, which result from impact with the opu (which clearly can be heard).
Up till now, the coexistence of solutions has merely been shown as a function of the excitation frequency. However, this phenomenon is also a function of the excitation amplitudes. This is shown in figure 3.3, where the amplitude of excitation is changed, whereas its frequency is fixed at 50 [Hz].

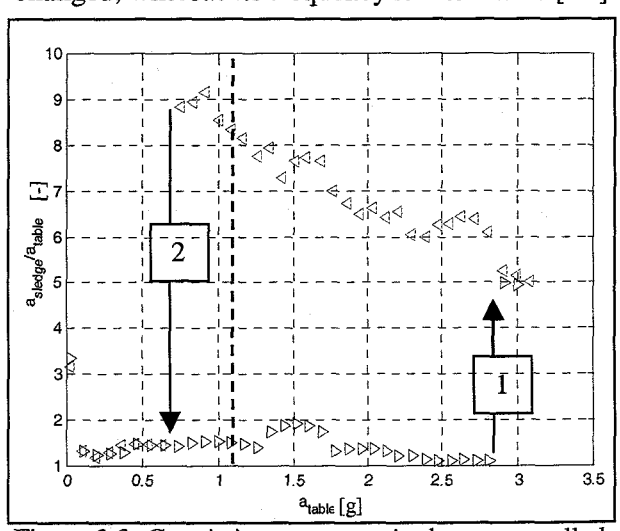

Figure 3.3: Coexisting responses in the uncontrolled case resulting from the non-linear opu dynamics by varying the amplitude of acceleration at a fixed excitation frequency of 50 [Hz].

In figure 3.3, the triangles again represent the direction of amplitude variation. Furthermore, it should be noticed that coexistence of solutions occurs at reasonably small levels of excitation (≥ 0.4 [g]), and therefore, is completely in range of the currently applied DOL measurements; see figure 2.12. As a last remark to figure 3.3 it is stressed that on the vertical axis the acceleration of the sledge is divided by the acceleration of the table, which obviously is not constant. This to prevent a misinterpretation when figures 3.3 and 3.4 are compared.
Both the frequency and amplitude dependency of the uncontrolled impact dynamics are depicted schematically in the following 3-dimensional figure; figure 3.4.

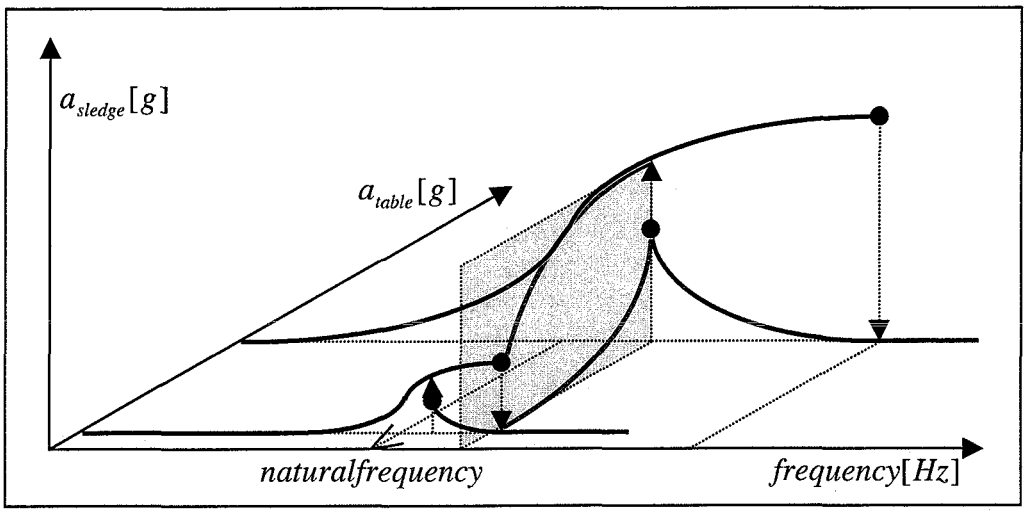

Figure 3.4: 3-d sketch of the uncontrolled situation around the natural frequency of the opu. The grey area and its red curves are a representation of figure 3.3. The thickened black curves are two representations of figure 3.1, where the first (smaller) one might be the one at the left of figure 3.1 and the second (bigger) one might be the one at the right.

This figure illustrates the complex behaviour encountered in the impact dynamics when varying only two system parameters: the excitation frequency and the amplitude of excitation.

So far, it has been shown that impact between opu and sledge occurs in the uncontrolled case. Whether there is impact or not can be heard. For two reasons, this has the potential of being the cause for mute in the controlled case:

1. Impact is encountered (in the uncontrolled case) in the frequency-range where an abnormal deviation from the DOL-curve is observed; see figure 2.12, and
2. Impact occurs at corresponding levels of excitation.

To investigate whether impact may be held responsible for the DOL deviation, a collision (impact) detection mechanism has been designed.

3.1.1 Design of a collision detection mechanism

To detect impact between the optical pick-up unit (opu) and the sledge in both the controlled and the uncontrolled case, an electric circuit has been designed, which allows for a voltage drop when the opu makes contact with either side of the sledge inner housing. The collision detection mechanism (CDM) can be represented by the electric circuit shown in figure 3.5 (see appendix 2 for more details).

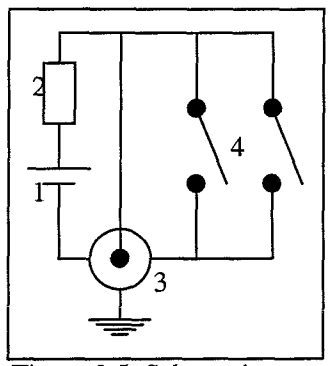

Figure 3.5: Schematic representation of the collision detection mechanism, with:
1. Battery; 2. Resistor; 3. Data acquisition system. One of the switches (4) is closed when the opu is in contact with the sledge.

By placing a detection wire, a small portion of the available cleavage has been consumed. This portion has been estimated at 9% by measuring the wire thickness. A drawback to this design of the CDM is its inability to differentiate between the two walls of the sledge inner housing.
Before investigating the controlled impact dynamics, the CDM has been applied on the uncontrolled impact dynamics. In the frequency-range between 35 [Hz] and 80 [Hz], impacts occurred and were registered. For the controlled case, the DOL-curve has been reconstructed with the CDM; see figure 3.6.

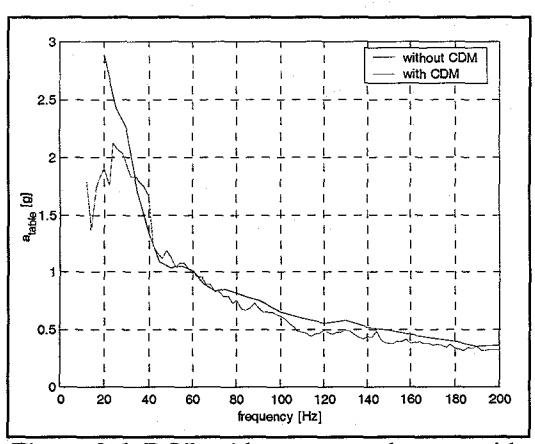

Figure 3.6: DOL with respect to the opu with the CDM (green) and without (blue).

Although figure 3.6 may lack the proper accuracy at frequencies below 20 [Hz] and beyond 80 [Hz], it clearly leaves the dip between 40 [Hz] and 60 [Hz] unaffected. For a particular time-series with impact, the output of the detection mechanism is shown for the uncontrolled case in figure 3.7.

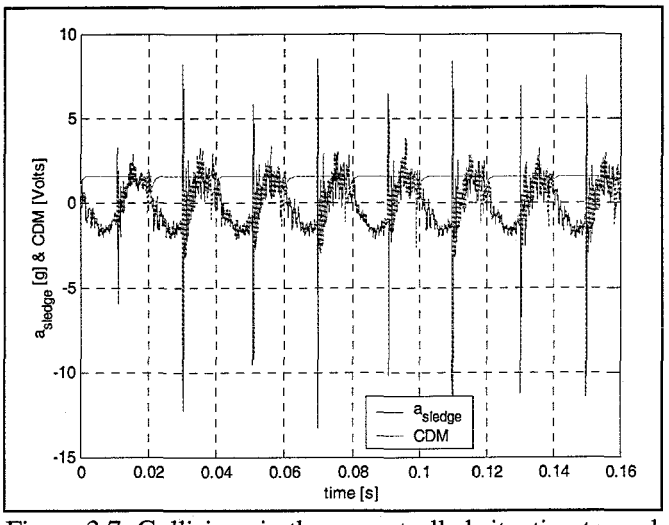

Figure 3.7: Collisions in the uncontrolled situation to evaluate the CDM by an external forced frequency of 50 [Hz] and an amplitude of the acceleration of the sledge of 1.1 [g].

By studying figure 3.7 with respect to figure 3.3 (at 1.1 [g]), it can be seen that the ratio between the maximum acceleration of the sledge and the maximum acceleration of the table is similar. It is mentioned that at this point in time the CDM was only applied at one side (which wasn't the case in figure 3.6, here it was applied at both sides). It is reasonable to assume that the CDM influences the impact dynamics between the opu and sledge, because where the CDM registers impact, it is not seen as clear in the acceleration signal of the sledge. On the other hand, if the opu is at rest (the opu is uncontrolled and there is no external disturbance), the cleavage at both sides of the opu is the same (it is positioned symmetric in radial direction with respect to the sledge). If an external sine-disturbance would be applied to the system and the opu starts colliding, it will collide with both sides of the sledge inner housing (which is clearly seen in figure 3.2).

3.2 IMPACT IN THE CONTROLLED CASE

With the CDM, mutes can be studied with respect to impact. In figure 3.8, such mutes are shown. A mute is detectable by the disturbance of the sine-shape in the radial error signal. The reason that the radial error doesn't become larger can be found in the fact that the distance between the lens and the nearest track (which might be a track other than the lens should follow) is taken as being the radial error. Here, the table is excited at a frequency of 50 [Hz] and has an acceleration amplitude of 1.12 [g] in both cases. For graphical purposes the acceleration of the sledge has been centred around the minus 2.5 axis instead of the horizontal axis.

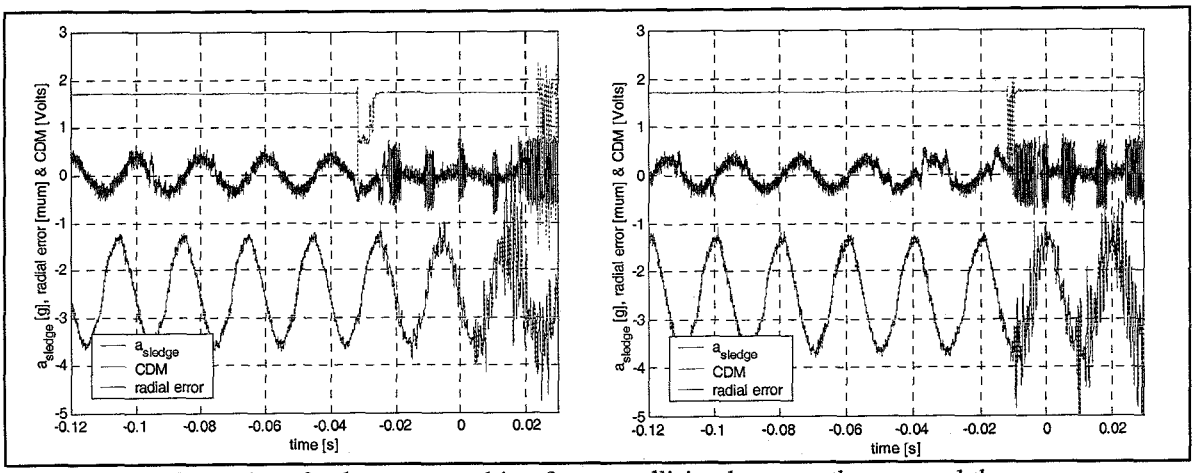

Figure 3.8: Examples of a dropout, resulting from a collision between the opu and the sledge. The table is excited with a frequency of 50 [Hz] and an acceleration amplitude of 1.12 [g] in both cases.

Apart from these experiments, several other experiments did show the occurrence of impact between 40 [Hz] and 60 [Hz] at an acceleration amplitude found as in figure 3.6. From these experiments, it has been observed that almost every mute related to impact resulted in dropout (i.e. the lens is not able to recover track and the module will stop playing, which can be seen because the disc stops spinning). One of the exceptions, however, is shown in figure 3.9 at an excitation frequency of 40 [Hz]. However, what can be seen in this figure (when comparing it with figure 3.8) is that the signal, generated by the CDM, doesn't reach zero. This means that, indeed, there was some contact between the opu and the sledge inner housing, but not as hard as in figure 3.8. So the opu moves extremely near towards the sledge inner housing, but not far enough to cause mute.

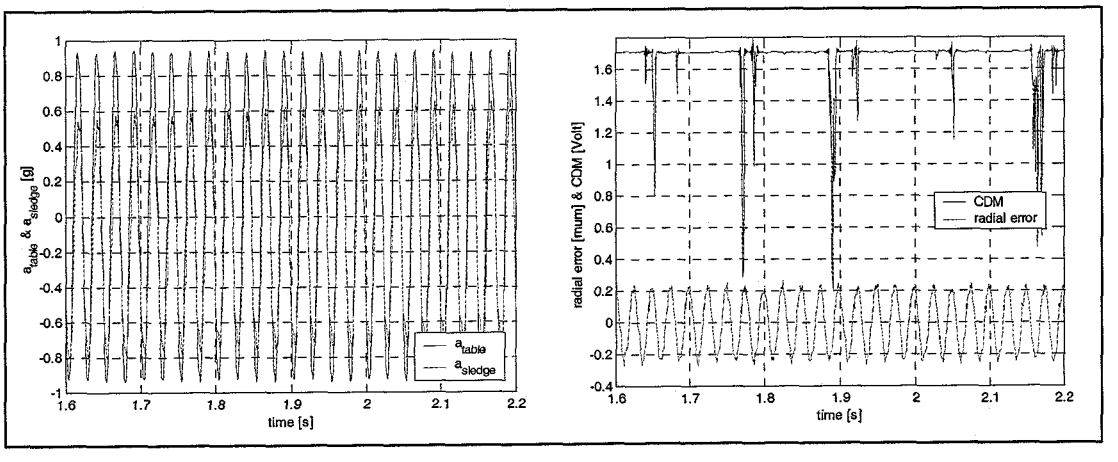

Figure 3.9: Contact between the opu and the sledge might occur in the controlled situation, without causing a mute. The table is excited with a frequency of 40 [Hz] and an acceleration amplitude of 0.9 [g].

Beyond 60 [Hz] the CD-player sometimes recovers from several mutes before it drops out by a mute related to impact. This is seen in figure 3.10, where the initial and the final mute (which results in a dropout) have been depicted at an excitation frequency of 96 [Hz]. This illustrates the idea that impact may complicate the re-

covery time after mute/dropout, but is not the reason to mute (obviously there are other causes for mute/dropout).

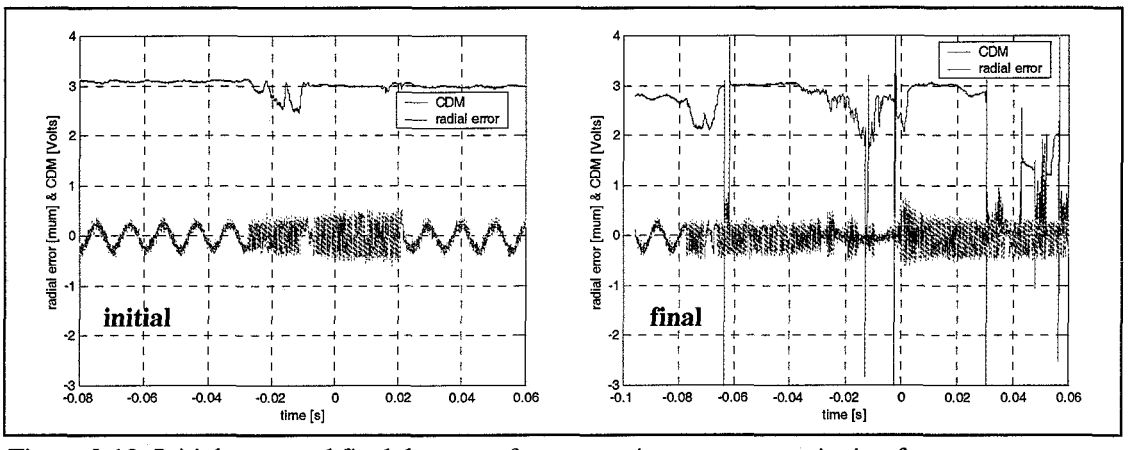

Figure 3.10: Initial mute and final dropout of two experiments at an excitation frequency of 96 [Hz].

Because the measurements were triggered, at which time is set to zero, the given time-scale is the one with respect to the trigger-moment. This remark is especially made with respect to figure 3.10.
Outside of the range of 40 [Hz] to 60 [Hz], mutes related to impact only occur occasionally. This wasn't expected because the dip (see figure 2.12) was expected to be a result of impacts found in the uncontrolled case (figure 3.1), and outside of this range no impacts occured in the uncontrolled case. In this study, only two experiments have been found that illustrate this phenomenon; see figure 3.11 at an excitation frequency of 110 [Hz] and 194 [Hz], respectively.

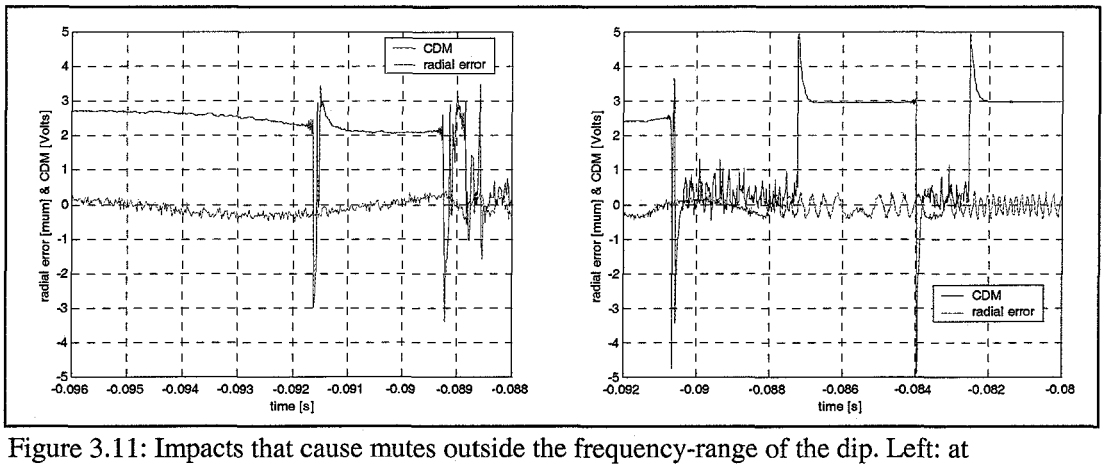

Figure 3.11: Impacts that cause mutes outside the frequency-range of the dip. Left: at an excitation frequency of 110 [Hz]; Right: at an excitation frequency of 194 [Hz].

The relation, regarding impact, between the controlled and the uncontrolled dynamics is unclear. This, because in the uncontrolled case no impacts occurred outside of the dip (found in the controlled case), i.e. in the uncontrolled case no impacts occurred above a frequency of 80 [Hz] at an acceleration amplitude lower than 2 [g] (see also figure 3.1). The dynamics in the controlled case have been changed drastically by control. To complicate even more, a discontinuity in the

maximum radial error signal has been observed in the controlled case. This is shown in figure 3.12.

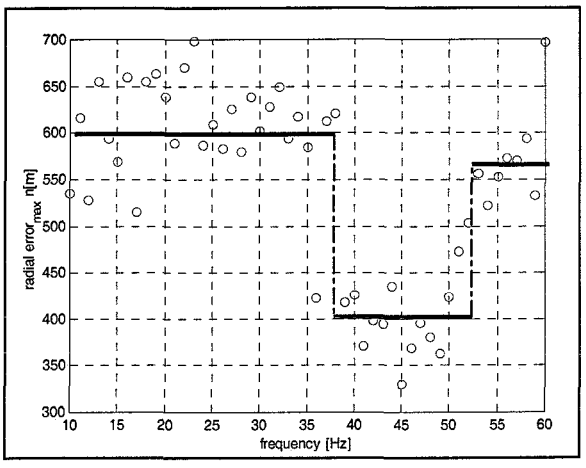

Figure 3.12: Not only in the curve of the DOL a dip can be seen, but also in the signal of the maximum radial error right before a mute (within the same frequency-range as the dip in the DOL).

Figure 3.12 shows that if the frequency of the excitation is higher than about 55 [Hz], the maximum radial error causing the system to mute approximately equals 560 [nm]. In the frequency-range around about 40 [Hz] to 55 [Hz], this is ≈400 [nm] and below this frequency-range it is ≈600 [nm]. The maximum radial error is obtained by increasing the amplitude of excitation up to a level where the CD-player mutes. The drop in the attainable radial error may be resulting from a tilt-mode of the opu (this mode has been determined in the past around 43 [Hz]). In figure 3.13 it is shown that when a tilt-mode occurs, a smaller maximum radial error can be registered, because the opu and sledge inner housing impact (due to the tilt-mode), where they shouldn't have (at this radial error) in the case that no tilt-mode occurred. In this case impact is related to the tilt-mode.
Another reason for the decrease in maximal attainable radial error, which is not related to impact, is found in the optics of the optical pick-up unit. For the measurement of both the radial- and the focus error, diodes are used. When the opu is not in torsion-mode, the diodes project a circle onto the disc (because the diodes create a signal perpendicular to the disc), which reflects the signals. If the opu is under a certain angle, with respect to the situation in rest (due to a tilt-mode), it means that also the diodes are under an angle. This means that the signal will not shine perpendicular onto the disc, so only part of the reflection will shine back onto the diodes. As a result the diodes receive to little of the returning signal and the CD-module drops out.

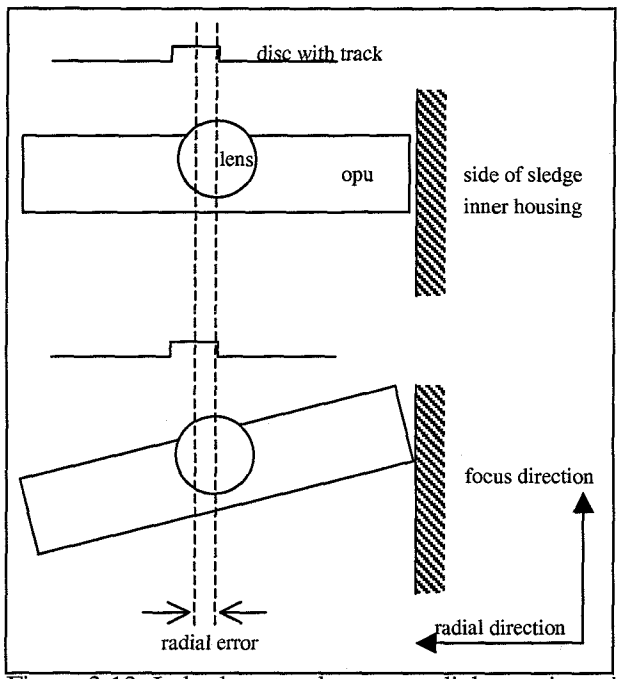

Figure 3.13: In both states the same radial error is registered. The opu above has no tilt-mode (and is able to have an even larger radial error, maximum radial error 560 [nm]) and is not in contact with the sledge inner housing, while the opu under is in contact (and is therefor not able to have a larger radial error, maximum radial error 400 [nm]).

3.2.1 Summary

- Between 40 [Hz] and 60 [Hz] excitation frequency it is very likely for a mute to be caused by impact between opu and sledge, this mute usually will result in dropout (see figure 3.8);
- It is possible for the opu to come near the sledge inner housing without causing mute/dropout (see figure 3.9);
- Beyond 60 [Hz] excitation frequency, if impact causes mute it will result in dropout (this phenomenon has an occurrence of 1% in the taken measurements; see figure 3.11);
- Outside of the frequency-range of the dip other causes for mute are much more important. However, it is mentioned that when during mute the opu and the sledge collide, the system will not recover and will dropout (see figure 3.10);
- It might be possible that the dip is caused by a tilt-mode. This opens up the possibility to have impact (between the opu and the sledge inner housing) without reaching the maximum attainable radial error (see figures 3.12 and 3.13). Also due to the optics of the opu the maximum attainable radial error might not be reached.

3.2.2 Concluding remarks

Although impact in the controlled case has been validated by measurement, it is not known where impact results from. Somehow, the opu impacts on the sledge, which may also occur due to poor sledge control, thus, the sledge impacts on the opu. To get more grip on the actual problem at hand, a parameter study will be performed in the next paragraph.

3.3 PARAMETER STUDY

The goal of this part is to investigate the influence of the uncontrolled dynamics on the controlled situation. Regarding equation 3.1, it is quit obvious that variance of opu mass and/or stiffness has the most influence to its behaviour. Furthermore, these two parameters are quit easy to change in the real CD-player. The goal of these variances is to increase/decrease the idea that the performance of the CD-player can be improved by influencing the mechanics of the CD-player. It should be noted that all experiments described in this section have been performed without the previously described collision detection mechanism.

3.3.1 Additional opu mass

By adding mass to the opu, the natural frequency of the opu will be decreased. Apart from the mass, also the modal damping is changed, namely:

$$\xi = \frac{b}{2\sqrt{km}} \qquad [2.2]$$

The expected effect of a mass addition on the non-linear behaviour of the opu near resonance is shown in figure 3.14.

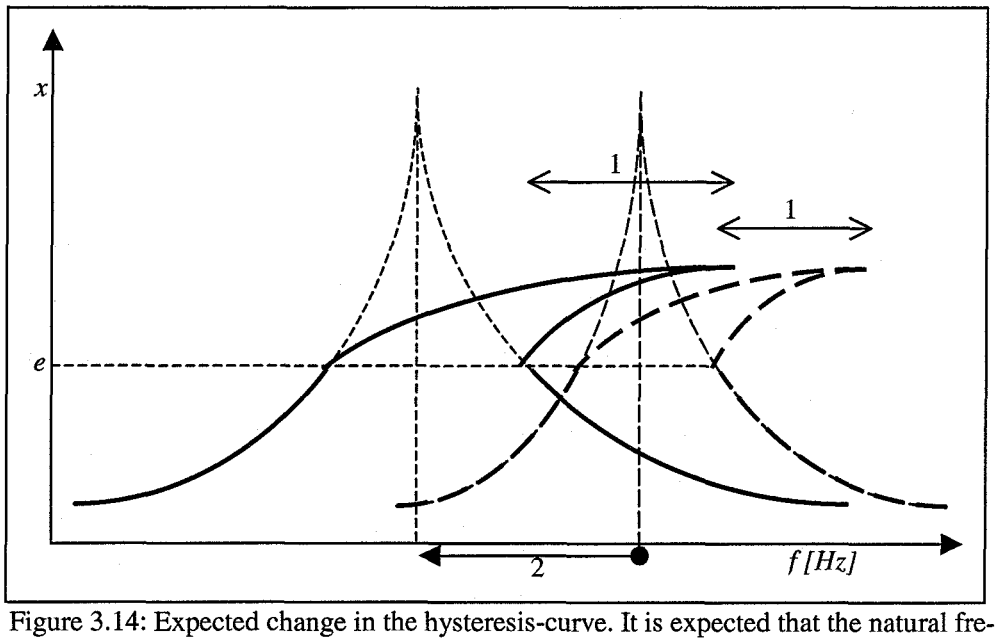

Figure 3.14: Expected change in the hysteresis-curve. It is expected that the natural frequency is shifted to a lower value (arrow *2*) and that the area of coexistence becomes larger (arrow *1*).

Namely, the area where the periodic solutions coexist (denoted by arrow *1*) is expected to increase due to the loss of damping, whereas it is shifted to lower frequencies due to the decreased natural frequency (denoted by arrow 2). In the experiment additional mass consisted of tin droppings on the opu, which increased the mass of the opu from $0.7 \cdot 10^{-3}$ [kg] to $0.9 \cdot 10^{-3}$ [kg]. In figure 3.15, the uncontrolled opu dynamics is shown for both values of the opu mass.

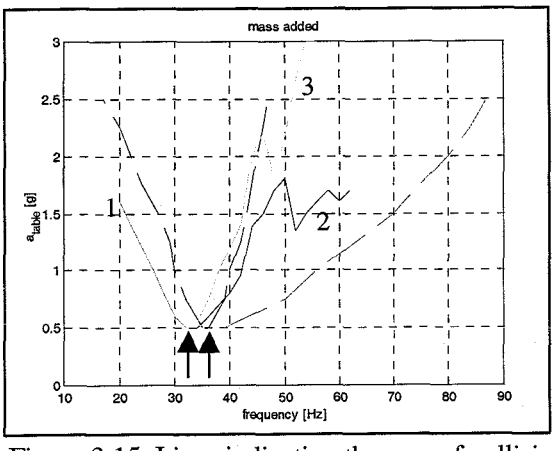

Figure 3.15: Lines indicating the area of collisions and the area of coexistence. This for the situation where mass is added to the opu (straight lines). Furthermore, as a reference, the original situation is also indicated (dotted lines).

The numbers in figure 3.15 (here denoted for the system with additional mass) correspond with the numbers in figure 3.1, which means that the natural frequency of the system should be found between line *1* and line *3*. Furthermore, and of greater importance, is that the area of coexisting solutions can be found between line *3* and line *2*. In figure 3.15 both the original (dotted) and the new (straight) lines are shown.
As can be seen in figure 3.15 the natural frequency is shifted from 34 [Hz] to 32 [Hz] (the right arrow indicates the natural frequency without additional mass, whereas and the left arrow indicates the natural frequency with additional mass). This represents a decrease of 6.4% (using formula 3.1, a decrease of 11.7% is expected). Furthermore, the area of coexisting responses has become smaller. These results do not solely match with an addition of mass so they should be interpreted carefully with respect to the controlled case. Looking at the original situation, it is expected that the dip will be found between line 3 and line 2. In figure 3.16, the results are shown for both the controlled and the uncontrolled case. Besides, in the right part of the figure both the DOLs with and without additional mass are depicted.

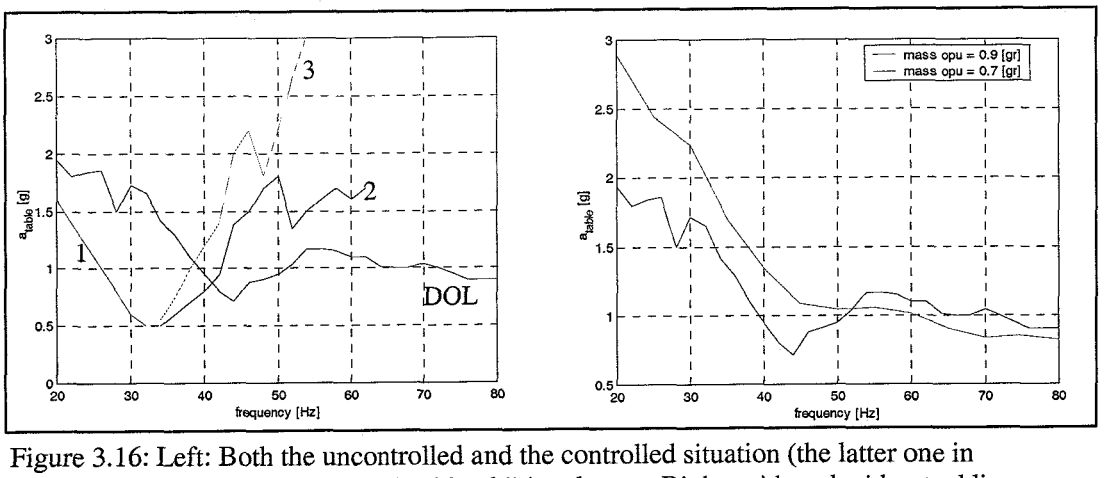

Figure 3.16: Left: Both the uncontrolled and the controlled situation (the latter one in the form of the DOL) with additional mass. Right: with and without additional mass in the controlled case.

It can be concluded that these curves show a deeper dip as before, but hasn't shifted significantly on the frequency axis such as expected from a mass addition. Again it is mentioned that these results should be interpreted carefully.

3.3.2 Additional opu stiffness

By stiffening the suspension wires of the opu, the natural frequency increased by a factor two, and so the modal damping has decreased by the same factor. For this reason, the stiffness of the opu has been increased from 32 [N/m] to 131 [N/m], which is an increase by a factor four. In figure 3.17, the impact dynamics for both values of the opu stiffness have been plotted (k=32 [N/m] and k=131 [N/m]).

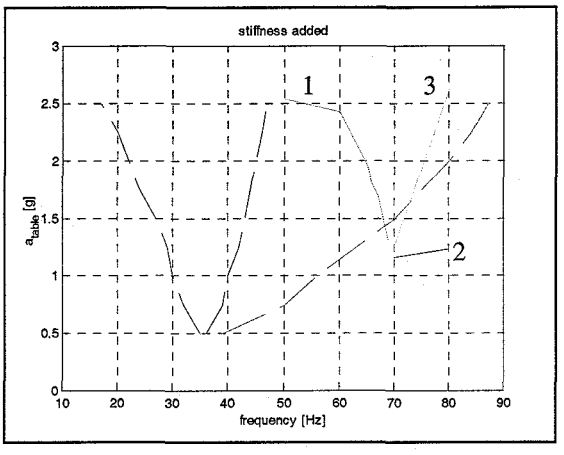

Figure 3.17: Lines indicating the area of collisions and the area of coexistence. This for the situation where stiffness is added to the suspension of the opu (straight lines). Furthermore, as a reference, the original situation is also indicated (dotted lines).

Figure 3.17 corresponds with the expectations, because the area of coexistence has become broader (with respect to the frequency). The level of acceleration must be chosen higher for the system to show impact. Namely, for the same amount of displacement between sledge and opu, additional force will be necessary when stiffness is added.

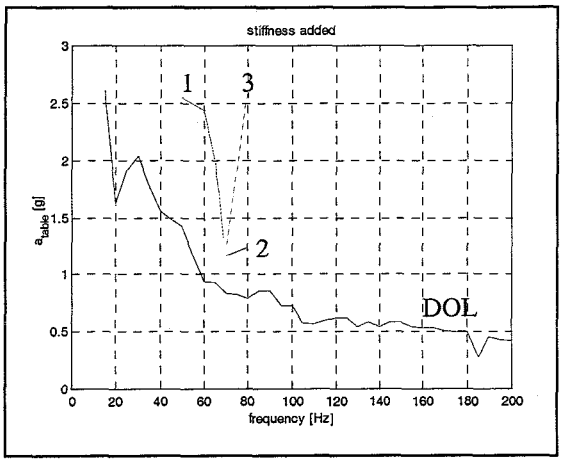

Figure 3.18: Both the uncontrolled and the controlled case (this in the form of the DOL) in the case that stiffness has been added to the suspension of the opu.

The centre of the dip in the DOL is shifted from 45 [Hz] to 70 [Hz], where also the new linear natural frequency is found. One key-observation, however, is the fact that no impacts have been encountered in the controlled case. From an uncontrolled point of view, this has been expected since the acceleration level for impact, see figure 3.18, is simply too large to be reached by the DOL-curve at the frequency-range where impact occurs. Thus, impact from an uncontrolled point of view cannot occur. This is why again there will be looked at the tilt-modes in the following paragraph.

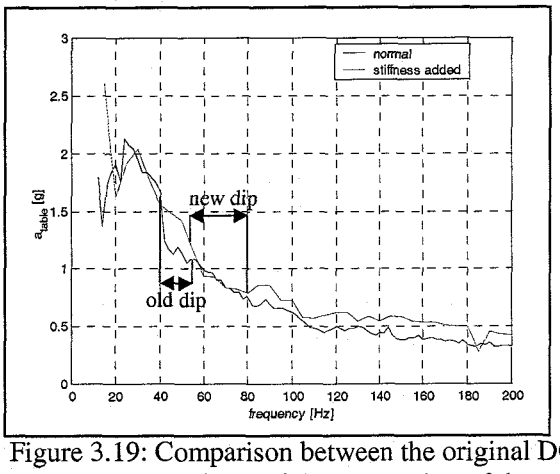

Figure 3.19: Comparison between the original DOL (blue) and the DOL in which the stiffness of the suspension of the opu has become a higher value (green).

In figure 3.19, the DOL-curves are shown for both values of the radial stiffness (k=32 [N/m] and k=131 [N/m]). The increase of the stiffness of the opu seems to result in an increase of performance beyond 80 [Hz]. Basically, this is an unexpected result, because the controlled stiffness (radial direction) is not influenced.

3.3.3 Reducing the degrees-of-freedom of the opu

An additional change to the mechanics of the optical pick-up unit is the restriction of the torsion-mode. Figure 3.20 shows a schematic representation of this mode. Note that in the impact dynamics of the opu, this mode has been neglected.

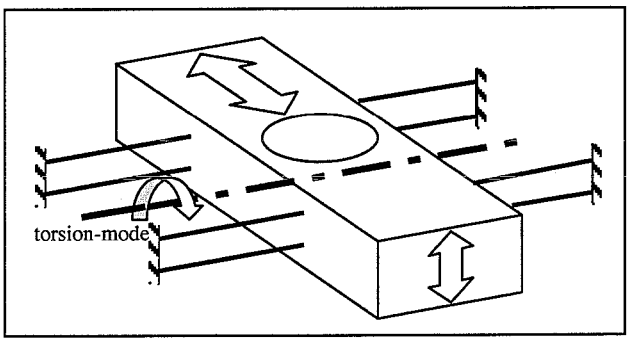

Figure 3.20: Schematic representation of the opu suspension, with its degrees-of-freedom.

To study the influence of this mode, with respect to the dip in the DOL-curve, its dynamics should be altered, without influencing the remaining dynamics. To do so, a bridge-construction, such as shown in figure 3.21 has been applied.

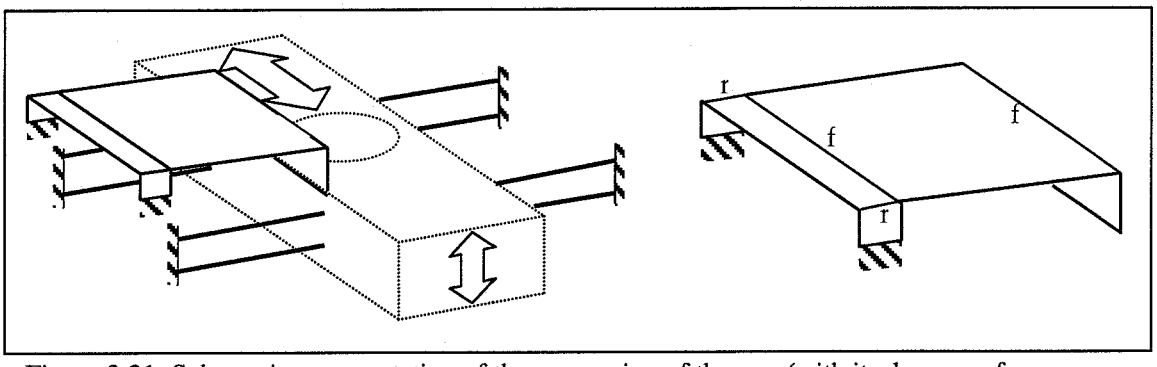

Figure 3.21: Schematic representation of the suspension of the opu (with its degrees-of-freedom), but now for the situation where the torsion (or tilt)-mode is suppressed.

The connections denoted by '*f*' in the right part of figure 3.21 allow for free translation in focus direction, whereas, the connections denoted by '*r*' enable free motion in radial direction.
With the bridge-construction, first the uncontrolled case has been examined. Surprisingly, no impacts between 0 [Hz] and 200 [Hz] have been found. So, or apparently a large radial stiffness has been introduced, or the torsion-mode played a more dominant role than expected. The controlled case is shown in figure 3.22, where it can be noticed that, within the given frequency-range, the dip is gone.

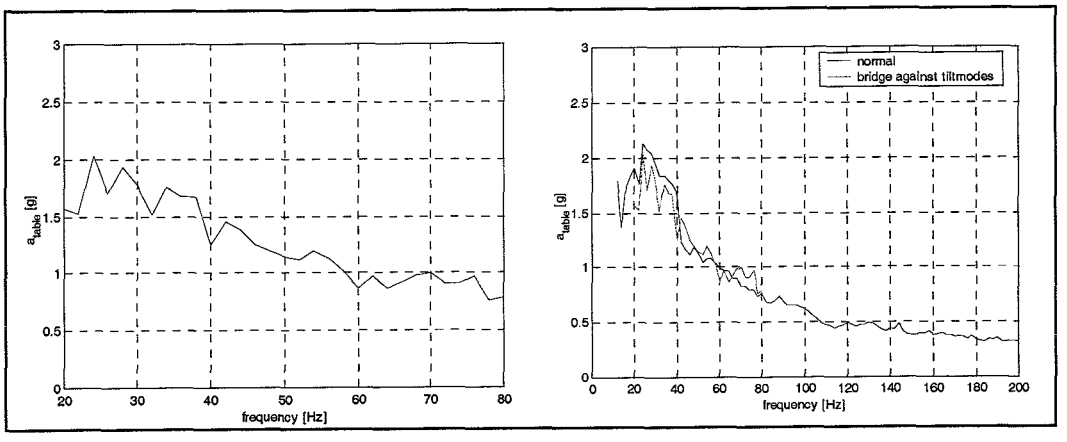

Figure 3.22: Left: DOL of the situation where the torsion (or tilt)-mode is suppressed. Right: with and without bridge-construction.

The disappearance of the dip in figure 3.22 doesn't necessarily indicate that the dip is a result of the tilt-mode (being at 43 [Hz]) in the original system, because also the radial stiffness may have been changed.
It is recommended that in order to reduce the number of degrees-of-freedom, another construction should be designed, which introduces no extra stiffness in both the radial and the focus direction.

4. Sledge dynamics

In the previous chapter, we mainly focussed on the opu-dynamics, which could be related to the dropout irregularities around 40 [Hz]. Here, the focus lies on the sledge dynamics, which will be related to the part of the DOL-curve between 60 [Hz] and 200 [Hz]. First, a model of the sledge dynamics will be provided. Second, for the uncontrolled system, the non-linear dynamics related to the pretension of the spindle will be studied without explicitly considering the controlled case. Third, disturbances of the sledge due to disc rotations will be related to the DOL-curves. Basically, it is shown that adaptation of the sledge dynamics may yield a performance increase. Finally, it is also shown that the voltage of the sledge motor plays a role of importance in the performance of the CD-player.

4.1 MODEL OF THE SLEDGE DYNAMICS

In order to gain information on the dynamics regarding the sledge, a simplified model has been constructed to estimate its natural frequencies. This model, which is only based on a few masses and stiffnesses, gives insight in the CD-player-dynamics in a rather straightforward manner. Nevertheless, there are three mayor drawbacks:

1. The model is limited in its degrees-of-freedom;
2. The model parameters may be difficult to estimate;
3. Non-linear components like cleavage, impact and pretension are neglected.

4.1.1 A simplified sledge model

The model is depicted in figure 4.1.

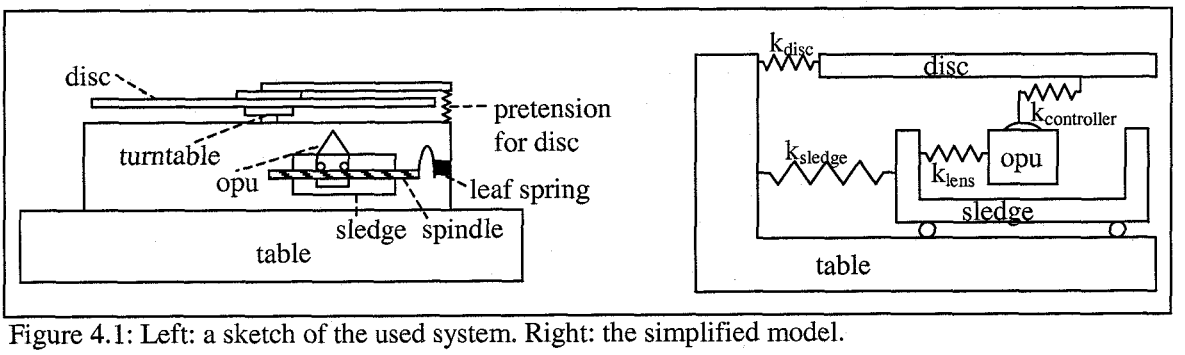

Figure 4.1: Left: a sketch of the used system. Right: the simplified model.

It consists of a few masses and springs; for reasons of simplicity, dampers have been omitted. The values of the spring stiffnesses and the masses are given in table 4.1 and 4.2 respectively; see also appendix 4 for the methods used for the estimation of these stiffnesses.

Stiffness	Value [N/m]
k_{disc}	$14 \cdot 10^3$
k_{sledge}	$280 \cdot 10^3$
k_{lens}	32.34
$k_{controller}$	$54 \cdot 10^3$

Table 4.1: Used stiffness values.

Mass	Value [kg]
m_{table}	6.8
m_{sledge}	$12 \cdot 10^{-3}$
m_{lens}	$0.7 \cdot 10^{-3}$
m_{disc}	$15 \cdot 10^{-3}$

Table 4.2: Used mass values.

The resulting equations of motion can be written as:

$$\begin{bmatrix} m_{table} & 0 & 0 & 0 \\ 0 & m_{sledge} & 0 & 0 \\ 0 & 0 & m_{lens} & 0 \\ 0 & 0 & 0 & m_{disc} \end{bmatrix} \ddot{x} + \begin{bmatrix} k_{disc}+k_{sledge} & -k_{sledge} & 0 & -k_{disc} \\ -k_{sledge} & k_{sledge}+k_{lens} & -k_{lens} & 0 \\ 0 & -k_{lens} & k_{lens}+k_{controller} & -k_{controller} \\ -k_{disc} & 0 & -k_{controller} & k_{disc}+k_{controller} \end{bmatrix} x = 0$$

$$or \quad M\ddot{x} + Kx = 0, \quad with \quad x = \begin{bmatrix} x_{table} \\ x_{sledge} \\ x_{lens} \\ x_{disc} \end{bmatrix}$$

[4.1]

Its natural frequencies yield:

Frequency [Hz]	Caused by ...
35	The opu suspension
151	Disc/turntable
770	The sledge suspension
1431	The controller

Table 4.3: Natural frequencies (resulting form the model depicted in figure 4.1) and the sub-systems causing it for the controlled situation of the model.

In figure 4.2, it is shown that some of these frequencies can be measured approximately on the set-up. In this figure, the frequency response function is shown of the acceleration of the sledge with respect to the acceleration of the table.

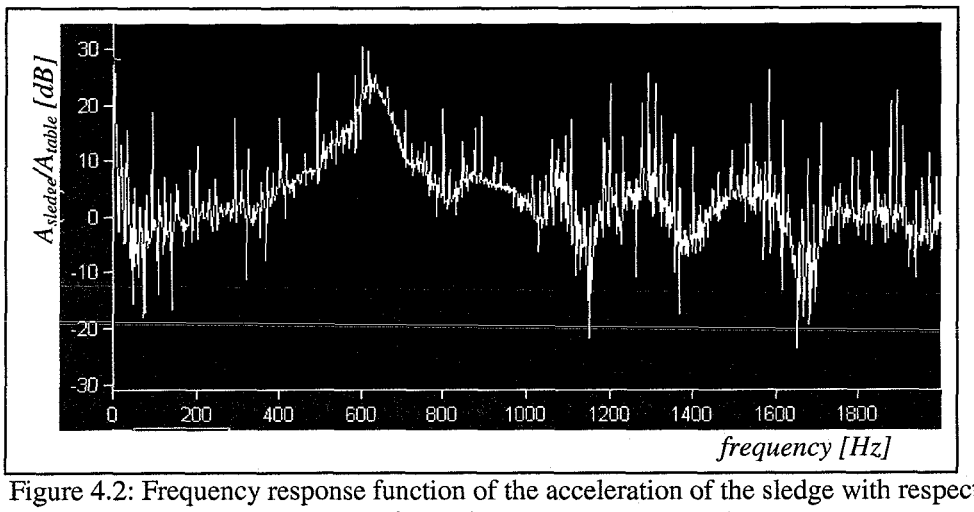

Figure 4.2: Frequency response function of the acceleration of the sledge with respect to the acceleration of the table.

By comparing the frequencies of table 4.3 with the ones depicted in figure 4.2, it is seen that resonance near 700 [Hz] and 1500 [Hz] seems to be related to the sledge suspension and the controller bandwidth, respectively. However, several other resonances remain. Therefore, three other, possibly non-linear, phenomena will be studied in the next paragraphs. These phenomena are: non-linear sledge dynamics, disc rotation and sledge motor voltage.

4.2 ON THE NON-LINEAR SLEDGE DYNAMICS

Basically, the suspension of the sledge represents a highly non-linear system containing play, pretension, etcetera. This is shown in figure 4.3.

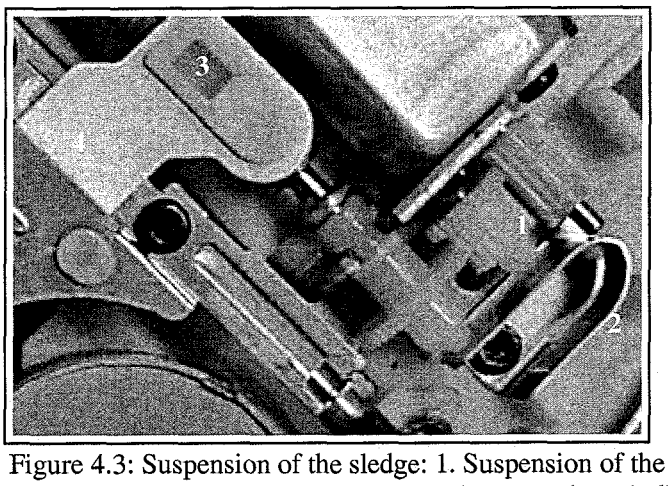

Figure 4.3: Suspension of the sledge: 1. Suspension of the gears; 2. The pretensioning leaf spring; 3. Suspension between the spindle and the nut; 4. Suspension of the nut and the sledge.

The pretensioned leaf spring is of special interest. Namely, a natural frequency (probably the one caused by the leaf spring) is found at about 530 [Hz] where, in the uncontrolled case, a number of coexisting solutions have been found in the experiments; see figure 4.4. Different from the coexisting solutions as studied in chapter 3, it can be seen in figure 4.4 that the branches (indicating the area of coexistence) bend to the left.

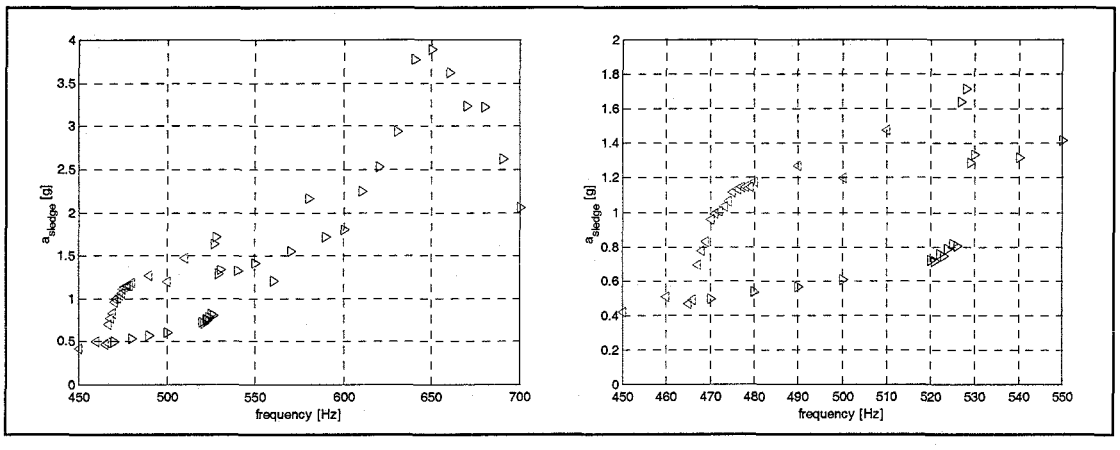

Figure 4.4: Periodic, coexisting solutions in the uncontrolled situation, resulting from the non-linear dynamics of the suspension of the sledge. With a constant amplitude of the acceleration of the table of 0.4 [g]. At the right an exploded view has been shown of the area of periodic coexisting solutions.

This can be seen by the triangles, which point out the direction of the frequency variation (blue a frequency increase and green a frequency decrease). A possible explanation for this observed phenomenon might be the fact that once the pretension force has been exceeded, the effective stiffness decreases (first the stiffness of the housing followed by the stiffness of the leaf spring). Contrary to the impact case of chapter 3, where an increase of effective stiffness occurred beyond certain amplitude levels of disturbance corresponding with a resonance peak that bended to the right. It should be noted that the acceleration levels, at which this phenomenon occurs, are fairly low such that the occurrence of this phenomenon in the controlled case can reasonably be expected. For some reason, however, in the controlled case, this phenomenon has not yet been observed. For more theoretical background to this phenomenon the reader is referred to appendix 3.
Besides the non-linear phenomenon around 500 [Hz], figure 4.4 also shows resonance at 650 [Hz]; see also figure 4.2. This natural frequency probably results from the sledge suspension between nut and sledge. Note that the acceleration level of the sledge at the maximum value of this peak is approximately ten times as high as the acceleration level of the table. So, suppressing this resonance will probably improve the performance of the CD-player.

4.3 IMPROVED SLEDGE DYNAMICS

As indicated, in the previous section, changes to the sledge dynamics may yield improvements to the CD-player performance. Hereto, additional stiffness has been applied between the nut and the sledge to suppress sledge resonance. The corresponding DOL-curve has been depicted in figure 4.5.

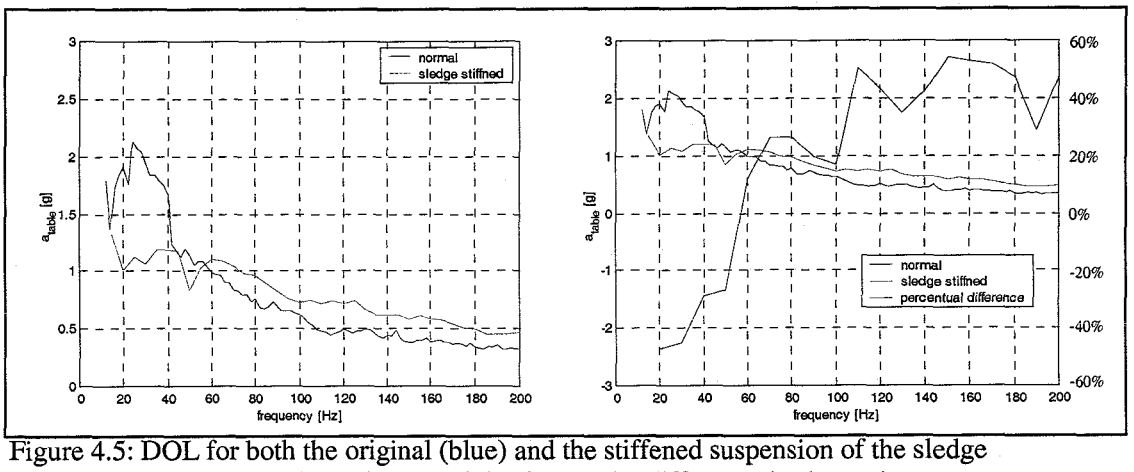

Figure 4.5: DOL for both the original (blue) and the stiffened suspension of the sledge (green). In the right part of the figure, the difference is shown in percentages (see the axes values at the right).

It can be seen that the module has improved about 30% to 50% beyond 60 [Hz], for which a proper explanation still lacks. Below 60 [Hz] the module has deteriorated which can be expected, because an increase in stiffness yields a better disturbance transmission.
With the additional stiffness, mute time-series have been measured such as depicted in figure 4.6. A closer look at these time-series (see for an example again figure 4.6 in the down right corner) reveals a 3150 [Hz] frequency contribution. Moreover, in the mute time-series of the previous DOL (the one without the increase of the sledge suspension stiffness) a 1560 [Hz] component was found instead of 3150 [Hz]. It should be noted that the excitation frequency, used to excite the table, is not equal in the two cases (156 [Hz] and 98 [Hz]). However, beyond 60 [Hz] excitation all experiments either showed the 3150 [Hz] component or the 1560 [Hz] component. So, it can be concluded that occurrence of both components is independent from the frequency of excitation.
In the following section, this phenomenon will be related to disc rotation.

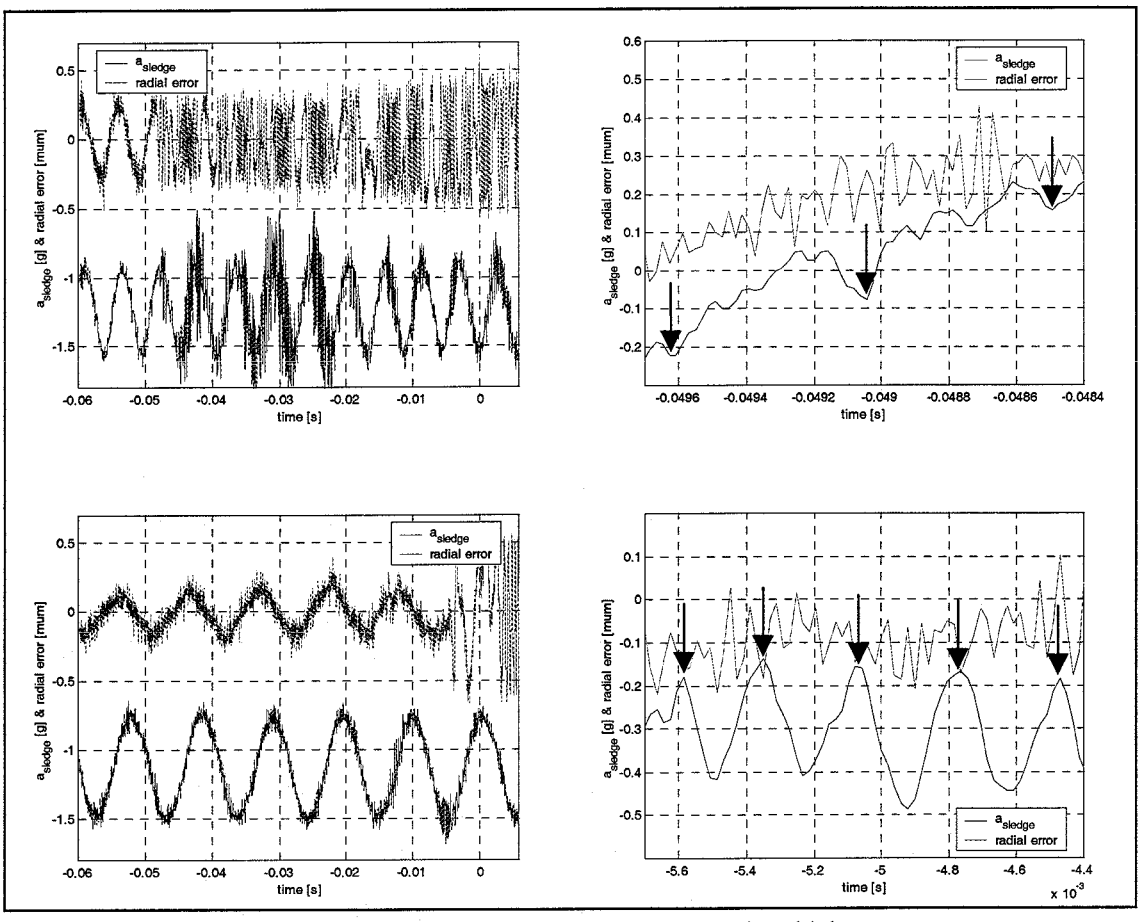

Figure 4.6: At the left two measurements are shown. Above, one in which a response frequency of 1560 [Hz] is found right before a mute and beneath one in which a response frequency of 3150 [Hz] is found. At the right an exploded view is shown of both signals, with the indicated response frequency. Furthermore it is pointed out that the signal of the acceleration of the sledge should have its vertical centre around the horizontal axis instead of minus 1.2.

4.3.1 Dynamics related to disc rotation

For the controlled case, figure 4.7 shows FFTs (fast Fourier transformations) of the sledge acceleration at different rotation speeds of the disc. It can be seen that an important frequency contribution is shifted from ≈3150 [Hz] via ≈2400 [Hz] to ≈1900 [Hz], by changing the track (on the disc).

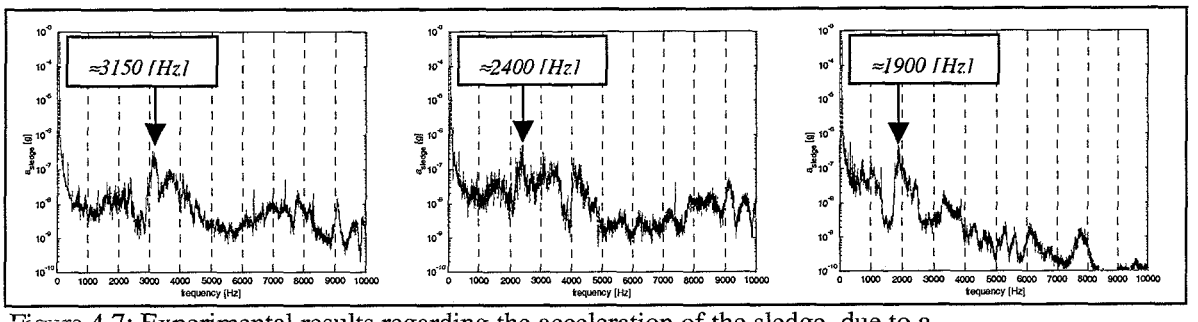

Figure 4.7: Experimental results regarding the acceleration of the sledge, due to a change of track. At the left track 1, in the middle track 10, and at the right track 20. The excitation frequency is 70 [Hz] and has an acceleration level of 0.5 [g].

In figure 4.7 it is seen that the disc dynamics (especially its rotational velocity) influence the sledge dynamics in a way, which is not yet explainable, but which unfortunately does influence the performance of the CD-module.

4.4 SLEDGE MOTOR VOLTAGE

The sledge motor voltage also contributes to the performance of the CD-player in the frequency-range of interest. This is shown in figure 4.8, where time-series entailing dropout are shown after exciting the CD-player at 156 [Hz]. Note that a sudden increase of the sledge motor voltage initiates a mute which yields dropout.

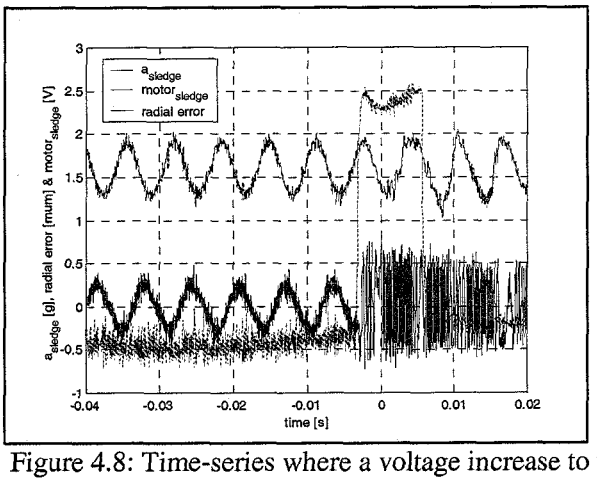

Figure 4.8: Time-series where a voltage increase to the motor of the sledge has been observed giving dropout.

The sledge motor voltage suddenly increases (for no known reason) with an amount of 3 [volts], which indicates a rather sudden movement of the sledge.
Here, this phenomenon has not been further studied. For a more detailed study, the reader is referred to [CTB556-01-6084, page 19].

5. Conclusions and recommendations

5.1 CONCLUSIONS

In this report, it has been shown that the dropout level (DOL)-curve can be viewed as the inverse process sensitivity function of the closed-loop. Then, irregularities from the thus obtained DOL-shape can either be attributed to non-linear dynamics or to unmodeled linear dynamics. Namely, the process sensitivity function is based on a single-degree-of –freedom linear model. Here, the non-linear opu dynamics have been studied to explain a large irregularity in the DOL-curve near 40 [Hz]. This irregularity is denoted as the dip. At other frequencies, irregularities have been considered mainly with respect to sledge dynamics. The main conclusion of this study can be summarised as follows.

With respect to the opu dynamics (chapter 3)

- Impact between the opu and the sledge has been measured in both the uncontrolled and controlled case in the vicinity of the natural frequency of the suspension of the optical pick-up unit (opu), i.e. the uncontrolled dynamics. These impacts are an important cause for mutes between 40 [Hz] and 60 [Hz] excitation frequency. Outside of this frequency-range impact also difficults recovery from mute and thus enlarges the probability of dropout;
- A dip in the maximum attainable radial error, i.e. the radial distance between the lens and the track, has been measured between 37 [Hz] and 55 [Hz]. At 37 [Hz], the attainable error instantly dropped from ≈600 [nm] to ≈400[nm]. At 55[Hz] it returned instantly to ≈560 [nm]. The instant character of the thus obtained dip heavily complicates an explanation based on a linear resonance phenomenon. However, a possibility for the instant decrease and increase respectively might be explained by the optics in the opu;
- To suppress tilt-modes, i.e. torsion-modes of the opu suspension, a bridge construction has been developed to add stiffness in the torsion direction, without influencing the dynamics in both the radial and the focus direction. With this construction the dip disappeared. However, from the uncontrolled dynamics it followed that the radial stiffness might have been increased. This made the conditions of the experiment somewhat suspicious, and, thus, its conclusions.

With respect to sledge dynamics (chapter 4)

- By stiffening the sledge suspension between the nut and the sledge the performance of the CD-player increased with 30% to 50% beyond 60 [Hz] excitation frequency. Unfortunately, however, below 60 [Hz] the performance decreased;
- At different tracks, an important frequency component in the sledge dynamics shifts. It is thought that the rotational velocity of the disc is of importance with respect to this frequency component in the non-linear sledge dynamics.

5.2 RECOMMENDATIONS

With respect to the opu suspension, the following recommendations are given:

- It might be possible to change the stiffness of the suspension of the opu by some sort of additional controller. In doing this, one might distinct two possibilities, being:
  1. If the system is excited in a certain range of frequencies, it might be possible to place the dip outside of this range;
  2. Another possibility might be to place the dip outside of the frequency-range of 0 [Hz] to 200 [Hz]. In this situation it costs lots of energy to displace the opu with respect to the sledge, because of the strong increased stiffness (natural frequency increases from 34.2 [Hz] to 205 [Hz] means an increase of the stiffness of the suspension of the opu from 32.34 [N/m] to 1164 [N/m], so the force, and thus the energy, given by the actuators should be 36 times higher).
- It is recommended to do further investigation into the tilt-modes, maybe by improving the used bridge construction. This improvement should only increase the stiffness in the direction of torsion and should not influence the directions of translation (radial and focus). This to see whether the dip decreases in the maximum attainable radial error;
- Perhaps it is possible to increase the cleavage. In doing this, it might be possible to prevent the sledge and the optical pick-up unit to collide.

With respect to the suspension of the sledge, the following recommendations are given:

- Stiffen the suspension even more (the suspension between the nut and the sledge), to see if again the system is improved. It is also not certain what happens when the stiffness of the suspension of the sledge is being decreased and the frequency-component (3150 [Hz]) is placed within the bandwidth of the controller. It might be possible that the controller is able to correct the frequency-component, although the flaw (the frequency-component) is a pure mechanical one.
- With respect to the voltage applied to the sledge motor, further investigation is recommended, because its share to the DOL is relevant.

List of related literature

[CTB556-01-6084] M.F. Heertjes, G.P.M. van Hattum, L.F. Koorneef & D. Biloen. (2001). *Error-mute relationship and non-linearity investigations in a Car CD/DVD drive, CFT Research Activities 2000.*

[CTB593-00-4174] F.L.M. Cremers, G.P.M. van Hattum. (2001). *Acceleration Feed Forward in CAR CD, CFT Research Activities 1999.*

Nomenclature

Quantity		Unit	
acceleration	a	meters per second gravitational acceleration	$[m \cdot s^{-1}]$ $[g]$ ($1\ [g] = 9.81\ [m \cdot s^{-1}]$)
damping	b	Newton second per meter	$[N \cdot s \cdot m^{-1}]$
constant	c	dependent on its meaning	*Unknown*
distance	d	meter	$[m]$
radial displacement	d_{rad}	meter	$[m]$
cleavage	e	meter	$[m]$
radial error	e_{rad}	meter	$[m]$
frequency	f	Hertz	$[Hz]$
natural frequency	f_n	Hertz	$[Hz]$
stiffness	k	Newton per meter	$[N \cdot m^{-1}]$
stiffness (of the controller)	k_p	Newton per meter	$[N \cdot m^{-1}]$
damping (of the controller)	k_d	Newton second per meter	$[N \cdot s \cdot m^{-1}]$
mass	m	kilogram	$[kg]$
time	t	second	$[s]$
voltage	v	volt	$[v]$
relative displacement	x	meter	$[m]$
differential action	D	second	$[s]$
load	F	Newton	$[N]$
integral action	I	Hertz	$[Hz]$
mass moment of inertia	J	kilogram squared meter	$[kg \cdot m^2]$
momentum	M	Newton meter	$[N \cdot m]$
proportional action	P	-	$[-]$
damping (dimensionless)	ξ	-	$[-]$
integrator action	τ_i	Hertz	$[Hz]$
rotation speed	ω	radians per second	$[rad \cdot s^{-1}]$

List of frequently used abbreviations

APM-Wetzlar :	Automotive playback modules in Wetzlar (Germany)
CDM :	Collision detection mechanism
DOL :	Dropout level
FFT :	Fast Fourier transformation
FRF :	Frequency response function
FT :	Fourier transformation
Opu :	Optical pick-up unit

Appendix 1:

Specifications of the shaker

To vibrate the table, a shaker is used. The shaker is a vibration exciter, Bruel & Kjær (B&K): type 4808, series 933348.

A1.1, SPECIFICATIONS SHAKER (LITERATURE)

Only literature with respect to the B&K type 4809 was found, which will be given. The shaker is a compact, permanent magnet electro dynamic exciter with a force rating of 44.5 [N] for vibrating small vibration test specimens at frequencies ranging from 10 [Hz] up to $20 \cdot 10^3$ [Hz]. Its moving coil has a nominal impedance of 2 [Ω] with a maximum current rating of 5 [A (rms)]. With assisted air cooling the maximum current and force rating may be extended up to 7 [A (rms)] and 60 [N] respectively. In table A1.1 some additional information is given with respect to the specifications of the shaker.

Description	Parameter
First axial resonance	$20 \cdot 10^3$ *[Hz]*
Maximum bare table acceleration	*75 [g] (100 [g] with air cooling)*
Maximum displacement (peak-to-peak)	$8 \cdot 10^{-3}$ *[m]*
Maximum velocity	*1.65 [m/s]*
Dynamic weight of moving element	$60 \cdot 10^{-3}$ *[kg]*
Dynamic flexure stiffness	$12 \cdot 10^3$ *[N/m]*

Table A1.1: Literary specifications shaker.

A1.2, SPECIFICATIONS SHAKER (EXPERIMENTAL)

To gain some experimental information on the shaker, a FFT of the acceleration of the shaker has been made. This FFT is the signal of the output of the shaker (the disturbance which the shaker transfers to the shaker-table) when its input is a chirp (a sine with increasing and decreasing frequency), with a frequency-range of 0 [Hz] to $20 \cdot 10^3$ [Hz], generated by siglab. To measure the FFT of the shaker, the shaker was decoupled of the table. The FFT of the decoupled shaker indicates the working-range of the shaker, so it is of minor influence to the results. In figure A1.1 the FFT of the shaker is shown.

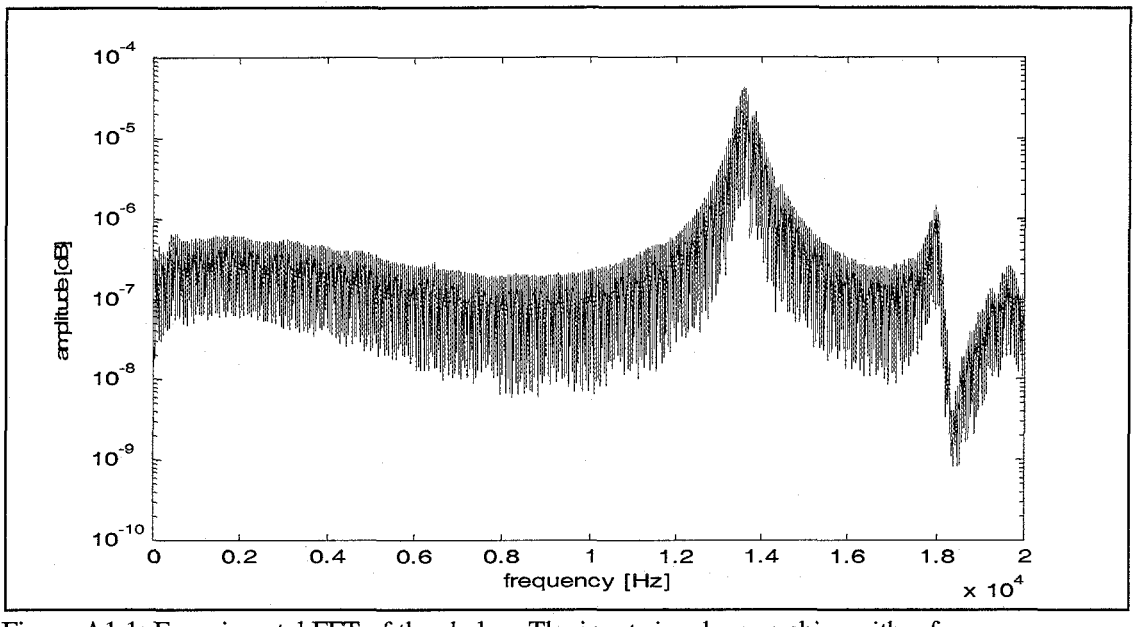

Figure A1.1: Experimental FFT of the shaker. The input signal was a chirp with a frequency-range of 0 [Hz] to $20 \cdot 10^3$ [Hz], the bandwidth was $20 \cdot 10^3$ [Hz], which is the maximum bandwidth for the used siglab-system.

The working-range is being decreased from $20 \cdot 10^3$ [Hz] (given by the manufacturer) to about $13 \cdot 10^3$ [Hz] (here the shaker has its first resonance-frequency, as can be seen in the FFT above).

Appendix 2:

Design of the collision detection mechanism

To investigate whether the optical pick-up unit and the sledge collide in both the uncontrolled and in the controlled situation, a collision detection mechanism (CDM) had to be developed.
One advantage of the collision detection is that not only collisions between the opu and the sledge can be detected, but it can also stop the actuator so that it doesn't burn through (this possibility has not been used in this study). There are several methods to detect collisions between the opu and the sledge. First, one can hear the collisions (audio). This can not be recorded with great precision, but can be used to validate another detection mechanism. Second, an electric circuit can be closed during the collision. The voltage can be recorded with great precision. A disadvantage in this method is that the dynamics of the system might be changed (which might not be the case). Third, a mechanical method can be found, the opu can push a switch, but this will probably highly influence the dynamics of the collision. There will now be looked at the second method. Six sub-methods have been found. One might notice that the optical pick-up unit (opu) is made of an isolating material and the side of the sledge is not, this can information be used in the detection method.

First a package of demands will be formulated:
1. The dynamics of the existing system may not be influenced;
2. Existing electronic fields are not to be influenced;
3. The lens must be free, so it can detect a track at all times;
4. It must be possible to remove the detecting mechanism without destruction of the system.

A2.1, MECHANICAL METHODS

In the next figures the three prime mechanical methods are shown, also pro's and con's will be discussed.

- Sub-method 1:

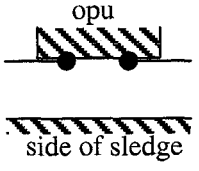

+ Can be done without isolating any further;
+ Little loss of cleavage between the sledge and the opu;
- Introduces some extra stiffness to the opu;
- Both wires have to make contact to detect a collision;
- When both sides are detectable, four wires have to be dealt with, without influencing the opu.

- Sub-method 2:

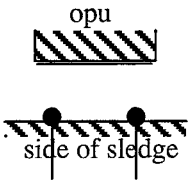

+ Introduces no extra stiffness to the opu;
- The side of the opu has to be made conductive, which introduces extra damping;
- The side of the sledge has to be isolated and the two wires decrease the available cleavage greatly;
- Both wires have to make contact to detect a collision.

- Sub-method 3:

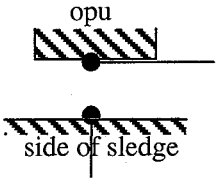

+ Can be done without isolating any further;
+ Little loss of cleavage between the sledge and the opu;
+ Wire to the sledge can be put on the outside of the opu;
- Introduces some extra stiffness to the opu (but not as much as sub-method 1);

In all the sub-methods regarded above there is very little space (half a millimetre) to place the detection method, which has to be placed with great accuracy.
There has been chosen for sub-method 3, because there is little loss of cleavage and it doesn't matter in what way the opu and the sledge collide.

A2.2, ELECTRICAL CIRCUIT

The other part of the mechanism is the electric circuit. Here there are two possibilities, being:

- Sub-method a, the circuit is being closed.

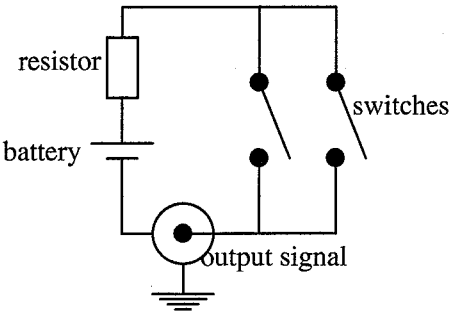

When both the switches are open no voltage is being measured by the siglab-system. When one of the switches is closed, the circuit is closed and a voltage is being measured.

- Sub-method b, the circuit is being shortcut.

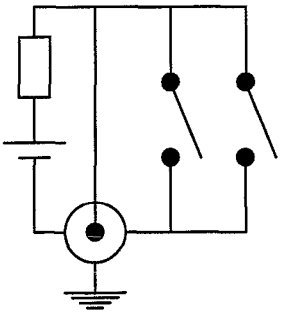

When both the switches are open a voltage is measured. If one of the switches is being closed, the circuit is shortcut and no voltage is being measured.

A2.3, CHOICE FOR THE FINAL COLLISION DETECTION MECHANISM

There is chosen for the last method, because whatever happens when one of the switches is being closed no voltage will be measured. Furthermore both sides are introduced on the same electric circuit (as shown in both the figures above), so there is no loss of output-channels (with respect to the siglab-system). A disadvantage of this is that one can not remark which side collides when one observer looks at the signal. Furthermore, the total loss of cleavage was estimated at 9%.

Appendix 3:

Theoretical background of periodic, coexisting solutions

A3.1, IN THE CASE OF CLEAVAGE

If a body exceeds its available cleavage and as a result it collides with another body, there will be a change in stiffness, with respect to the movement of the first body. This change of stiffness explains the appearance of coexisting solutions. This will be explained with the help of figure A3.1.

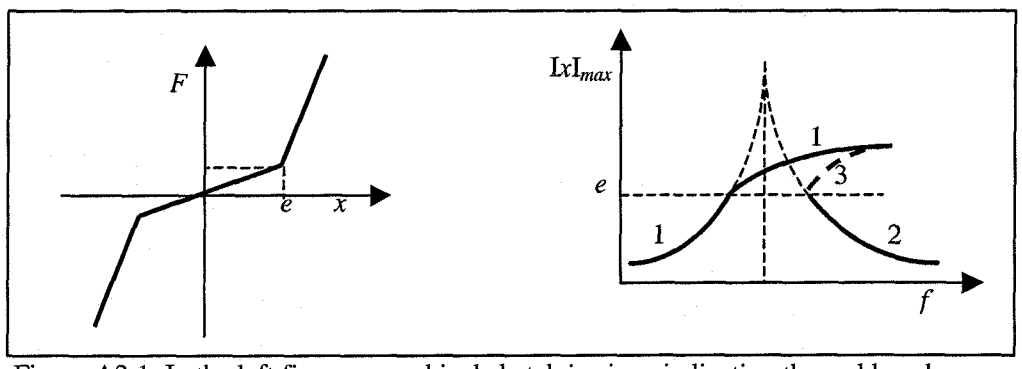

Figure A3.1: In the left figure a graphical sketch is given indicating the sudden change in stiffness. In the figure at the right the non-linear dynamic result is sketched. In these figures 'x' is the relative displacement of the opu with respect to the sledge, 'e' is the maximum relative displacement without contact, 'F' is the force used to displace the opu and 'f' is the frequency of the externally applied harmonic excitation.

In figure A3.1 at the left, the change in stiffness is seen. Starting at the origin and following the line with increasing relative displacement between the opu and the sledge (x), the opu collides with the sledge at point '$x = e$'. Here the stiffness increases discontinuously. In the figure at the right one sees that (following the path with increasing frequency, f, denoted as path 1) when the point '$x = e$' is reached, the natural frequency becomes higher due to an increase in the stiffness. As a result the curve bends and this path is followed until it becomes unstable and the solution drops to the path below (path 2). This instability is due to the fact that if the path 2 (in the figure at the right) would be followed with decreasing frequency (starting at a frequency above the frequency of the drop) up until the point '$x = e$' it would theoretically be possible to have a third, unstable, solution (here denoted as path 3). At a certain point path 1 and path 3 intersect, at which path 1 becomes unstable. Since it is practically impossible to follow path 3, only two solutions will be found

experimentally. Following path 2 with decreasing frequency, it can only be followed again up to the point '$x = e$'. After this the solution 'jumps' to the path above (path 1) and the area of coexistence is found. If a line is drawn in the figure at the right which indicates the maximum relative displacement ('e'), as it is done in the figure, one can find the linear natural frequency somewhere in the middle of this line (between the two branches below '$x = e$').
By doing this, the natural frequency has been validated for the suspension of the opu, because in all cases the natural frequency lies between *30 [Hz]* and *40 [Hz]*.

A3.2, IN THE CASE OF PRETENSION

Now some theoretical background to the phenomenon regarding pretension dynamics (with a decrease of stiffness) will be given. It is expected that the branches, defining the area of coexistence, will bend to the left, due to the decreased stiffness (introduced by the leaf spring) of the suspension of the sledge. In the following this expectation will be explained schematically.

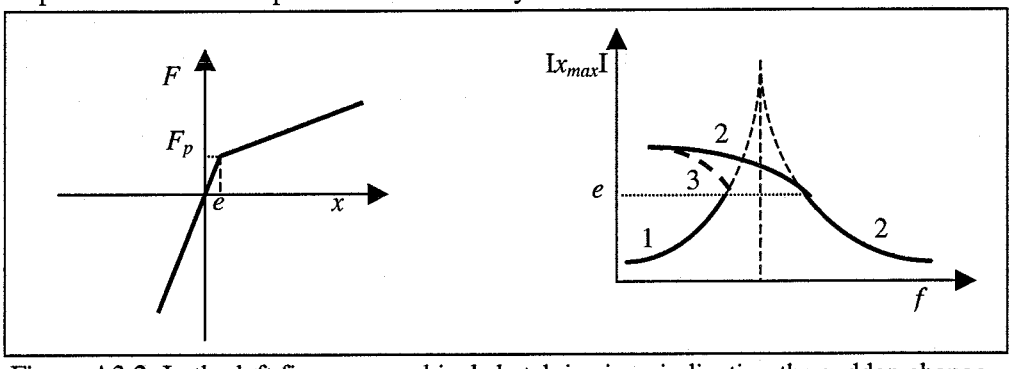

Figure A3.2: In the left figure a graphical sketch is given indicating the sudden change in stiffness. In the figure at the right the non-linear dynamic result is sketched. In these figures 'x' is the displacement of the sledge, 'e' is the maximum force without deformation of the leaf spring, 'F' is the force used to displace the sledge, 'F_p' is the pretension force of the leaf spring and 'f' is the frequency.

In figure A3.2 at the left, the change in stiffness is seen. Starting at the origin and following the line with increasing displacement of the sledge (x), the suspension of the sledge changes stiffness at point '$F = F_p$'. Here the stiffness decreases discontinuously. In the figure at the right the displacement of the sledge is placed on the vertical axes. In figure A3.2 at the right one sees that (following the path with increasing frequency, f, path 1) when the point '$x = e$' is reached, the natural frequency becomes lower due to a decrease in the stiffness. As a result the curve jumps at '$x = e$' and this path can be followed further. Following this path (path 2) with decreasing frequency, it can only be followed again up to the point where the path becomes unstable. The path 2 becomes suddenly unstable for the same reason as it has in section A3.1. After this the solution 'jumps' to the path beneath (path 1) and the area of coexistence is found. Because the relative movement between the spindle and the table becomes smaller, it might be possible that the path doesn't become unstable, but will smoothly follow the part into the other periodic solution. This is graphical explained in figure A3.3.

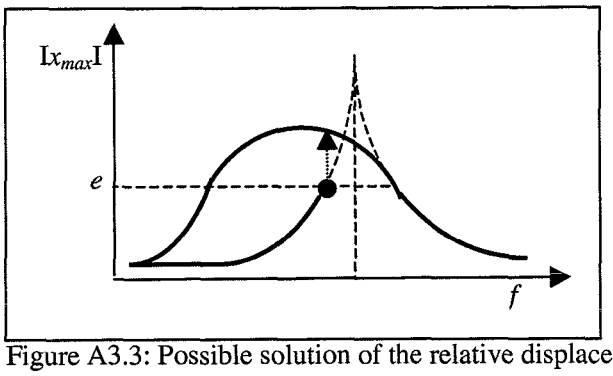

Figure A3.3: Possible solution of the relative displacement with respect to the frequency.

Appendix 4:

Estimation of important stiffnesses

Some stiffnesses are known due to literature or previous measurements, but others aren't. In this appendix all of the used stiffnesses will be dealt with.

A4.1, STIFFNESS BETWEEN THE DISC AND THE TURNTABLE

The stiffness between the disc and the turntable is estimated statically, by pushing the disc with a force-transducer (the force, F, can be measured) and measuring the relative displacement (d). The stiffness can now be estimated with the following formula:

$$k_{cd} = \frac{F}{d} \qquad [A4.1]$$

In doing so a stiffness of $14 \cdot 10^3$ [N/m] was found.

A4.2, STIFFNESS OF THE SUSPENSION OF THE SLEDGE

The stiffness of the suspension of the sledge is divided into two parts, being: the stiffness of the leaf spring and the stiffness between the spindle and the sledge.
The stiffness of the leaf spring is estimated dynamic, using two accelerometers. These meters are being placed at both sides of the leaf spring as can be seen in the next figure.

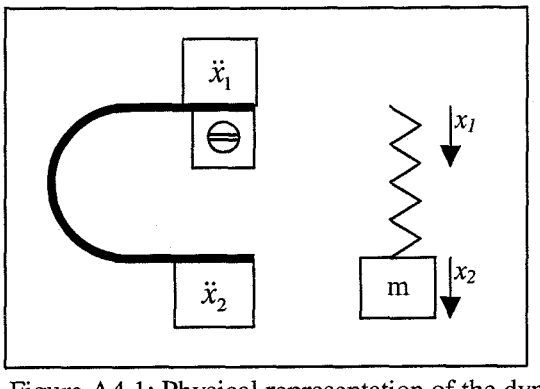

Figure A4.1: Physical representation of the dynamic measurements made on the leaf spring. $\ddot{x}_i$ (with i = 1,2) are the accelerometers.

Now one can make a dynamic model, resulting in the next expression:

$$m\ddot{x}_2 = k(x_1 - x_2) \qquad [A4.2]$$

Using $x_1 = \sin(2\pi ft)$ and doing the experiment below the natural frequency one can use $x_2 = A\sin(2\pi ft)$. Now dividing the function by x_2, the expression can be rewritten into:

$$k = \frac{4\pi^2 f^2 mA}{A-1} \qquad [A4.3]$$

In this A is the difference in amplitude between the two measurements made by the accelerometers, f is the used frequency and m is the mass of the accelerometer (being $0.6 \cdot 10^{-3}$ [kg]). This resulted in a stiffness of 550 [N/m].

The stiffness between the spindle and the sledge is estimated statically. Pushing the sledge with a force-transducer, measuring the relative displacement and again using formula A4.1, a stiffness of $280 \cdot 10^3$ *[N/m]* was found.

A4.3, STIFFNESS OF THE SUSPENSION OF THE OPU

Again two stiffnesses can be estimated (as already indicated in figure 3.7). The first one is found when the opu is not in contact with the sledge. The second one is the stiffness when the opu is in contact with the sledge (during a collision).
The stiffness of the suspension of the opu has been found in literature, being 32.34 [N/m]. This also has been validated using figure 3.1 and formula 3.1.
The stiffness of the suspension of the opu, during collision with the sledge, is estimated dynamically by using such a collision measured in the uncontrolled situation. During a collision there is loss of energy. A measure for this loss of energy is the closed surface given in figure A4.2.

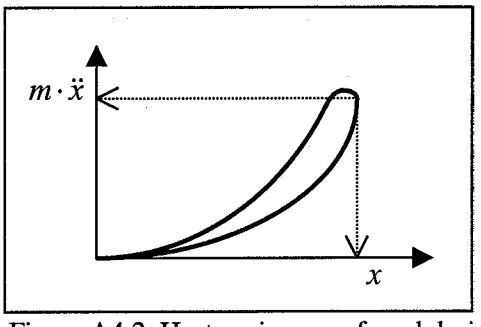

Figure A4.2: Hysteresis-curve found during a collision. The closed surface within the hysteresis-loop represents the energy-loss during the collision. The by the arrows indicated point, is the point of deepest impact (here the velocity is zero).

The mass used in this estimation, is the mass of the opu, which 'penetrates' the side of the sledge. It is mentioned that the found stiffness is not the stiffness for the side of the opu, but the stiffness of the contact. Using formula 3.1 and rewriting it into:

$$k = 4\pi^2 f^2 m, \qquad \text{[A4.4]}$$

a stiffness has been found of $5 \cdot 10^6$ [N/m].

A4.4, STIFFNESS OF THE CONTROLLER

The stiffness of the controller can be estimated using the bandwidth of the controller of the radial actuator. This bandwidth has been found being 1400 [Hz]. Taking the mass of the opu (being $0.7 \cdot 10^{-3}$ [kg]) and using formula A4.4, a stiffness for the controller has been found of $54 \cdot 10^3$ [N/m].

--o--o--o--